Environmental Science Processes & Impacts

ROYAL SOCIETY OF CHEMISTRY

PAPER

View Article Online
View Journal | View Issue





Cite this: *Environ. Sci.: Processes Impacts*, 2023, **25**, 1031

# The fate of organic peroxides indoors: quantifying humidity-dependent uptake on naturally soiled indoor window glass†

Marc Webb, [a] Liyong Cui,[a] Glenn Morrison,*[a] Karsten Baumann,[ab] Jason D. Surratt, [ac] Zhenfa Zhang,[a] Joanna Atkin[c] and Barbara J. Turpin *[a]

Humidity plays an important role in the surface removal and concentrations of indoor pollutants such as ozone; however, the indoor surface dynamics and chemistry of organic peroxides is largely unknown. Organic hydroperoxides (ROOHs) are known to participate in the multiphase chemistry of outdoor aerosols and clouds, suggesting that reactive uptake in condensed grime on indoor surfaces is plausible, particularly in humid homes. Here, the effect of relative humidity (RH) on the deposition velocity ($v_d$) and reaction probability ($\gamma$) of a model ROOH to naturally soiled indoor glass surfaces was investigated; specifically, by using authentic isoprene hydroxy hydroperoxide (1,2-ISOPOOH) as the model compound. Glass was soiled in 3 local homes for 1+ years and characterized. The removal of ISOPOOH by soiled and clean glass was measured under 5–6%, 56–58%, and 83–84% RH conditions using a novel flow reactor designed for indoor surfaces coupled to an iodide chemical ionization high-resolution time-of-flight mass spectrometer (I-HR-TOF-CIMS). The $v_d$ and $\gamma$ increased with increasing RH, ranging from 0.001–0.059 cm $s^{-1}$ and 0.4–4.6 ($\times 10^{-6}$), respectively, on soiled glass surfaces. The $v_d$ and $\gamma$ ranged from only 0.001–0.016 cm $s^{-1}$ and 0.1–0.8 ($\times 10^{-6}$), respectively, across RH conditions on clean glass, demonstrating a greater RH effect on soiled materials than clean. Loss rates calculated under humid conditions to soiled glass ($\sim$1–6 $h^{-1}$) were competitive in scale with ventilation rates in typical residences, indicating the importance of surface uptake for indoor ROOH concentrations. This work provides parameters for predictive modeling of indoor ROOHs. To our knowledge, these are the first direct measurements of the $v_d$ of an ROOH to naturally soiled indoor surfaces.

Received 1st February 2023
Accepted 2nd May 2023

DOI: 10.1039/d3em00041a

rsc.li/espi

### Environmental significance

The indoor environment is a major location for exposure to air contaminants. Organic hydroperoxides (ROOHs) are expected to be formed indoors and a better understanding of their indoor chemistry is warranted. This manuscript provides the first measurements of the humidity-dependent uptake of ROOHs on authentically soiled indoor surfaces, providing critical parameters needed to model the indoor dynamics of these reactive, water-soluble compounds. We found that humid conditions substantially enhanced the surface removal of ROOHs by soiled interior glass surfaces, but the same enhancement was not observed for clean glass surfaces. We discuss the potential for multiphase chemistry of ROOHs indoors, which could alter human exposure to indoor pollutants. The parameters provided will aid the accuracy of predictive indoor chemistry models.

## Introduction

Homes are major locations for human exposure to airborne chemicals[1,2] because people spend 70% of their time in homes, on average,[3] and limited ventilation[4,5] leads to elevated concentrations of compounds[2,6,7] emitted from indoor materials,[8] humans[9,10] and human activities.[11,12] Because of large indoor surface area-to-air volume ratios,[13] surfaces play a major role in modifying exposures,[14] increasing indoor chemical residence times[15] and mediating reactions that alter the airborne chemical mixture.[16–18] A quantitative understanding of indoor air–surface interactions for a variety of pollutants is critical to the development of predictive models for population exposure assessment, effective exposure mitigation strategies and improved built environment design.[19]

Material surfaces—painted walls, windows, flooring, furnishing *etc.*—are soiled with deposited particles and surface films[20,21] that contain low- and semi-volatile organic and

[a]*Department of Environmental Sciences and Engineering, Gillings School of Global Public Health, University of North Carolina at Chapel Hill, Chapel Hill, NC, USA. E-mail: bjturpin@email.unc.edu; glennmor@email.unc.edu*

[b]*Picarro Inc., Santa Clara, CA, USA*

[c]*Department of Chemistry, College of Arts and Sciences, University of North Carolina at Chapel Hill, Chapel Hill, NC, USA*

† Electronic supplementary information (ESI) available. See DOI: https://doi.org/10.1039/d3em00041a

inorganic species[22–24] emitted directly from sources (primary)[20] and formed through indoor chemistry (secondary).[25–28] Surface films can enhance the sorption of water from humid air[22] and undergo hygroscopic growth.[29] This provides a reservoir for moisture and partitioning of water-soluble organic gases (WSOGs) that may enable aqueous surface chemistry.[30,31] WSOGs (*e.g.* acetic acid; Henry's law constant or $K_H$: $4 \times 10^3$ mol $L^{-1}$ $atm^{-1}$)[32] are ubiquitous and abundant indoors, where they are known to decay at rates faster than air change rates (air changes $h^{-1}$; ACH) due to substantial surface removal, especially for more polar, oxidized WSOGs with larger $K_H$ values and smaller saturation vapor pressures.[31,33]

Organic hydroperoxides (ROOHs) are important atmospheric WSOGs and oxidants,[34,35] but their uptake by indoor surfaces is largely uncharacterized. Surface uptake is predicted to be the dominant sink for indoor hydrogen peroxide ($H_2O_2$),[36] and we expect the same may be true for ROOHs. Multifunctional ROOHs are more water soluble with $K_H$ values on the order of that of $H_2O_2$ ($10^5$ mol $L^{-1}$ $atm^{-1}$)[32,37–39] and have predicted saturation vapor pressures[40–42] that should favor deposition to surfaces,[33,43] especially in the presence of surface-associated water. ROOHs are known products from the oxidation of unsaturated compounds such as terpenes[34,44–47] and are predicted to exist in indoor air (*e.g.*, ozonolysis of limonene from scented cleaning products).[45,46,48] Indoor measurements of gas-phase ROOHs are limited to measurements of total hydroperoxides ($H_2O$ + ROOH) which 2 studies measured at mixing ratios up to ~2 ppb in simulated[45] and manipulated[46] indoor settings in the absence of cleaning. ROOHs are expected to be important reactive oxygen species (ROS) for which human exposures could result in negative health outcomes[49,50] and their chemistry could alter the composition of indoor air, particulate matter and surfaces through oxidation and partitioning.[50,51] Reactive uptake of ROOHs is already known to play an important role in the chemistry of outdoor aqueous aerosols and clouds.[37,52–56] For example, humidity, and presumably aerosol liquid water, was shown to facilitate the reactive uptake to aerosols of ROOHs derived from terpene ozonolysis.[53,55] Certainly differences between ROOH multiphase chemistry on surfaces in damp homes and on outdoor aerosols are expected, because differences in pH, hygroscopicity, phase separation and other critical properties are likely, although not adequately characterized. For example, aerosols are typically more acidic[57] than indoor surfaces are expected to be.[58] Taken as a whole, the existing evidence suggests ROOH multiphase chemistry in condensed grime is plausible indoors, where relative humidity (RH) is in the 30–70% RH range[59] and neutral to slightly acidic sorbed water is expected,[58] particularly in humid homes. While the indoor environment is likely a major location for surface chemistry and exposure to ROOHs, the dynamics and fate of indoor ROOHs are poorly understood.

Currently, there is a dearth of experimentally-derived uptake kinetics on real indoor surfaces for most indoor pollutants. Indoor surface deposition velocity ($v_d$; cm $s^{-1}$), which is a mass transfer coefficient that combines pollutant transport and uptake to a surface, as well as air changes per hour and surface area-to-volume ratio, are critical parameters for modeling indoor pollutant behavior.[60,61] These data are needed to validate and refine predictive models.[62,63] Quantifying ROOH uptake dynamics to soiled surfaces under a range of RH conditions can help improve predictive modeling of indoor ROOH exposures and prediction of indoor air chemistry, dynamics, and composition. The goal of this study was to measure the $v_d$ of a model organic hydroperoxide (*i.e.*, isoprene hydroxyhydroperoxide or ISOPOOH) to authentically-soiled impervious indoor surfaces (clean and soiled window glass) and investigate the impact of RH on surface removal. This study used a novel parallel plate flow reactor to measure the uptake dynamics of the 1,2-ISOPOOH isomer (2-hydroperoxy-2-methylbut-3-en-1-ol), which was synthesized in-house, at 5–6%, 56–58% and 83–84% RH to window surfaces that were clean and authentically soiled in 3 homes (Houses A–C). The percent removal, molar uptake, $v_d$ and reaction probability of ISOPOOH ($\gamma_{ISOPOOH}$) by glass surfaces under the range of RH conditions will be discussed. The reactor performance was validated, in part, by performing ozone ($O_3$) experiments on clean glass (at 2%, 54%, 94% RH) and comparing deposition velocity and reaction probability to literature values.

## Materials and methods

### Parallel plate flow reactor

Wall-coated cylindrical glass flow reactors or flow tubes coupled to mass spectrometers have been used extensively to measure gas uptake to aerosols. Coatings either served as a protective film to minimize wall-loss (or reaction) of semi-volatile gases in the presence of aerosol flow (*e.g.* halocarbon wax)[64–67] or a supportive film to mimic uptake to aerosols.[68,69] In this work, a novel flow reactor (Fig. 1) with a parallel plate geometry and easily changeable walls was designed, characterized, and used instead of a traditional aerosol flow tube, to accommodate typical surfaces found in indoor environments, which are often flat (*e.g.*, glass, painted drywall, wood, metal). The reactor was designed with dimensions and gas residence times typical of cylindrical glass flow tubes where gas uptake to walls was observed.[64,65,68,69] Deposition velocities and reaction probabilities for $O_3$ and 1,2-ISOPOOH to clean and authentically soiled glass window plates were determined using the flow reactor coupled to an $O_3$ monitor (OM) or an iodide chemical ionization high-resolution time-of-flight mass spectrometer (I-HR-TOF-CIMS), respectively. Flow reactor experiments are listed in ESI Table S1.†

The flow reactor was constructed from anodized aluminum (UNC BeAM Design Center) and all interior surfaces were Teflon coated (URG Corp, Chapel Hill, NC). The reactor contains a laminar flow chamber (interior volume: 1 m × 0.1 m × 0.02 m) that holds two removable 1 m × 0.1 m glass plates in parallel 0.02 m apart and an upstream mixing chamber. $O_3$ or 1,2-ISOPOOH mixed in RH-conditioned air flow (2.5–4 L $min^{-1}$ mass flow) was directed into the 0.08 × 0.15 × 0.08 m mixing chamber. The mixing chamber exit is tapered to 20 $cm^2$, which restricted flow and promoted mixing, and then passed through a mesh flow straightening screen (Fig. S1b–d†). A movable sampling tube (ESI Section 2 and Fig. S1†) facilitated

 

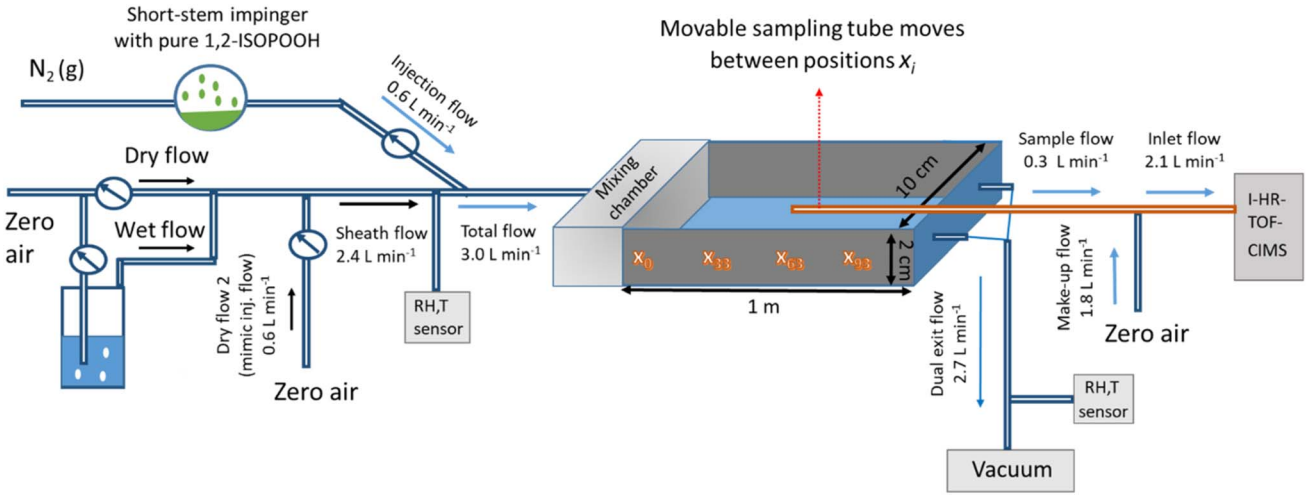


Fig. 1 Parallel plate flow reactor schematic and experimental set-up for 1,2-ISOPOOH measurements. 1,2-ISOPOOH was mixed with dry or humidified air and continuously injected through a fixed delivery port.

measurements of $O_3$ or 1,2-ISOPOOH decay due to surface removal with increasing distance along the flow reactor, corresponding to increasing interaction times between the gas and the parallel surfaces. The sampling line was coupled to an $O_3$ monitor (960 to 1000 $cm^3$ $min^{-1}$; OM; 2B Technology Model 202; Boulder, CO) or an I-HR-TOF-CIMS (2.1 L $min^{-1}$; Aerodyne Research Inc., Billercia, MA). The I-HR-TOF-CIMS has been optimized for the detection of isoprene-derived oxidation products (including 1,2-ISOPOOH), as previously described in detail.[64,70,71] All flows were controlled *via* mass flow controllers except for the flow through the movable sampling tube (sample flow). The $O_3$ analyzer and I-HR-TOF-CIMS have fixed inlet flow rates that were coupled to the movable sampling tube. Because the I-HR-TOF-CIMS flow rate (2.1 L $min^{-1}$) is large relative to the total flow through the reactor (3 L $min^{-1}$), vacuum controlled exit ports were used to create a slight positive pressure system that forced 10% of the total flow through the movable sampling tube (0.3 L $min^{-1}$) before introducing a make-up zero air flow (1.8 L $min^{-1}$) before the I-HR-TOF-CIMS inlet (Fig. 1). Sampling positions of the movable sampling tube and concentrations at each sampling location are denoted as $x_i$ and $C_i$, respectively, where $i$ denotes the distance down the reactor from a starting position $x_0$ (cm); consecutive sampling positions were 15–33 cm apart at $i = 0$, 33, 63, or 93 cm or $i = 0$, 15, 30 or 45 cm for 1,2-ISOPOOH and $O_3$ experiments, respectively. Initial concentrations for $C_0$ were taken at the exit of the mixing chamber upstream of the glass surfaces for 1,2-ISOPOOH experiments to maximize distance between sampling positions, while $O_3$ measurements occurred over a shorter distance (approximately 40 cm) due to the rapid uptake of ozone; in both cases, the initial sampling position is denoted $x_0$ and concentrations are normalized by their value at $x_0$. Additional flow reactor details (*e.g.*, tabulated dimensions, flow rates, Reynolds numbers and boundary layer thickness), images, and the flow diagram for $O_3$ experiments are provided in ESI Section S2 and S3, including Fig. S1, S2 and Table S2†.

### Deposition velocity and reaction probability

The deposition velocity, $v_d$ (cm $s^{-1}$), describes the effective surface removal rate of gases and is defined by gas flux to a surface normalized by the gas-phase concentration in the bulk.[60,61] The mass balance model for deposition to parallel plates in flow reactors has been described many times in the literature and fundamental chemical engineering texts.[60,72–74] The slope of the measured natural log of the normalized gas signal in the reactor [$\ln(C_i/C_0)$] *vs.* distance in the direction of flow ($x$; cm) (or location of movable sampling tube) provides a pseudo-first order wall-loss rate coefficient ($k_{wall}$; $cm^{-1}$) used to calculate $v_d$ in eqn (1):

$$v_d = \frac{-Qk_{wall}}{2W} \quad (1)$$

where $Q$ is the volumetric flow rate ($cm^3$ $s^{-1}$) and $W$ is width of the parallel plates (10 cm). Mass transport of gas molecules to a surface followed by gas–surface interactions (partitioning or reactive uptake) are the two mechanisms involved in surface deposition. Therefore, $v_d$ can be mass transport-limited where surface resistance to uptake is negligible or surface reaction-limited where the surface is sufficiently resistant to uptake. Deposition velocity was modeled as two resistors in series by Cano-Ruiz *et al.*,[60] as shown in eqn (2):

$$v_d = \left[\frac{1}{v_t} + \frac{4}{\gamma\langle v\rangle}\right]^{-1} \quad (2)$$

where $\langle v\rangle$ is the Boltzmann velocity ($3.62 \times 10^4$ cm $s^{-1}$ for $O_3$), $v_t$ (cm $s^{-1}$) is the transport-limited deposition velocity and $\gamma$ is reaction probability. The, $v_t$ parametrizes gas mass transport to a surface with negligible resistance to uptake. Reaction probability or the reactive uptake coefficient, $\gamma$, parametrizes how likely gas–surface interactions result in surface reaction and is defined as the fraction of gas molecules colliding with a surface that are irreversibly removed from the gas phase. Reaction

probability can be calculated using eqn (2) if $\nu_d$ and $\nu_t$ for the specific gas and flow system are known.

### Ozone uptake experiments on glass surfaces

Since there is a large body of literature on $O_3$ uptake to indoor surfaces,[16,60] we began by measuring $O_3$ uptake to characterize the novel reactor and validate its performance. A lower bound uptake constraint under reaction-limited conditions was characterized by measuring $O_3$ $\nu_d$ values to halocarbon wax-coated glass plates where minimal uptake was expected. Halocarbon wax (Halocarbon Products Corp) coatings have been routinely used to minimize wall-losses from gas–surface reaction in glass flow tubes when investigating gas uptake to aerosols.[64] An upper bound uptake constraint under transport-limited conditions was characterized by measuring $O_3$ $\nu_d$ values to potassium iodide (KI)-coated surfaces where maximum uptake was expected (a "perfect sink"). KI-coated surfaces are known to be minimally resistant to $O_3$ uptake,[75] and have been used to measure $\nu_{tO_3}$ in a variety of systems.[76–78] The measured $\nu_{tO_3}$ in the presence of KI-coated surfaces was used to estimate the $\nu_t$ for ISOPOOH ($\nu_{ti}$) as explained below in Results: Transport-limited deposition velocity for $O_3$ and 1,2-ISOPOOH. The reactor performance was validated by measuring $O_3$ $\nu_d$ and $\gamma$ values to clean glass plates (at 5, 50 and 85% RH) where uptake was expected to fall between constraints and agree with reported values in literature. Details and procedures for ozone experiments are provided in ESI Section S3.†

### Preparation of authentically-soiled glass plates and other substrates

Cleaned glass window plates (1 m × 0.1 m) and glass microscope slides (0.075 m × 0.025 m) were deployed vertically, within 60 cm of the ceiling in locations where they did not receive direct sunlight, in the main living areas of 3 local homes for 20–24 months, for natural soiling. Glass substrates were deployed in the living room of House A (closed floor plan) and in the dining area of Houses B and C (open floor plan). Glass window plates were mounted to walls using large picture hanging adhesive strips (3M Command Strips). Standard glass microscope slides were propped vertically against the wall (forming 10° angle with the wall), supported by aluminum L brackets taped to the wall in the same area as the glass window plates. The soiled glass window plates were used for 1,2-ISOPOOH uptake experiments. Glass microscope slides were used to characterize the surface film morphology and surface loading of hygroscopic organic and inorganic species. Home RH, temperature, deployment dates and other details are reported in Table S3†. A detailed procedure for preparing the glass plates, halocarbon wax-coated glass and KI-coated painted drywall is found in ESI Section S4.† Painted drywall was selected as the KI coating substrate (perfect sink) because KI distributed more uniformly on that surface than on glass.

### Characterization of authentically soiled glass

Surface films on soiled glass microscope slides were analyzed by atomic force microscopy-infrared spectroscopy (AFM-IR) or extracted in water and analyzed for total water-soluble organic carbon (WSOC) using a total organic carbon (TOC) analyzer or organic and inorganic ions by ion chromatography (IC), as described in ESI Section S4.†

### 1,2-ISOPOOH experiments

1,2-ISOPOOH is the predominant ISOPOOH isomer produced under low-$NO_x$ conditions in outdoor air.[79–81] Furthermore, it is likely the most abundant semi-volatile and water-soluble ROOH found in outdoor air due to the large emissions (and reactivity) of isoprene globally.[82] 1,2-ISOPOOH ($C_5H_{10}O_3$) was selected as a model indoor ROOH because it is moderately water soluble ($K_H$: $1.8 \times 10^5$ mol $L^{-1}$ $atm^{-1}$ at room temperature),[39] undergoes multiphase chemistry in atmospheric waters[39] and an in-house synthetic standard was available. Detailed synthetic procedures for 1,2-ISOPOOH were previously provided by Riva *et al.*;[70] 1,2-ISOPOOH is produced with a purity of typically 95%. 1,2-ISOPOOH uptake experiments were conducted at 5–6%, 56–58% and 83–85% RH on clean glass plates, glass plates that were authentically soiled in 3 homes (House A, B and C), and halocarbon wax-coated glass plates. 1,2-ISOPOOH was stored at −30 °C and allowed to reach room temperature for one hour prior to use. For each experiment, the window glass-loaded reactor was first conditioned at the experimental flow rate and RH for 90 minutes. The RH at the reactor exit reached within 5% of the RH at the entrance within 30 minutes, indicating that the RH in the system had equilibrated ~1 hour before introduction of 1,2-ISOPOOH. 1,2-ISOPOOH was pipetted into a short-stem glass impinger (Gelman Instrument Company, no. 7202 with stem shortened) and introduced into the flow reactor by entraining the headspace gas in 0.6 L $min^{-1}$ ultra-high purity nitrogen gas ($N_2$) and then diluting the headspace flow with 2.4 L $min^{-1}$ house air. The 1,2-ISOPOOH flow (3 L $min^{-1}$) was continuously delivered to the RH-conditioned flow reactor at a fixed injection port at room temperature (22–25 °C). Injection and sampling of 1,2-ISOPOOH started simultaneously with the movable sampling inlet initially positioned at the upstream edge of the parallel glass plates at the mixing chamber exit, $x_0$. The sampling flow rate through the movable sampling tube was maintained at 0.3 L $min^{-1}$ and then diluted to 2.1 L $min^{-1}$ with house air before entering the low-pressure ion–molecule reaction (IMR) region (*i.e.*, ~80 mbar) of the I-HR-TOF-CIMS. The 1,2-ISOPOOH was detected as an ISOPOOH iodide cluster ($ISOPOOH \cdot I^-$) at the mass-to-charge ($m/z$) of 244.9 using I-HR-TOF-CIMS. Experiments were conducted by positioning the movable tube in each of 4 locations at increasing distances down the plates (*i.e.*, from short residence time to longer residence time and then repeating as shown in Fig. S3†). Distances of 0, 33, 63 and 93 cm ($x_0$, $x_{33}$, $x_{63}$ and $x_{93}$) were used in most experiments. The movable sampling tube began positioned at $x_0$ and was then withdrawn 33 cm to $x_{33}$, 30 cm to $x_{63}$, 30 cm to $x_{93}$, and then returned to the starting position ($x_0$). Stopping at each $x_i$, the movable sampling tube was stationary for 2–21 minutes (sampling time) at each position before moving to the next position. Sampling times were short (2 min) early in the experiment and gradually increased; measurements were

 

performed for 5.5 to 13.5 hours. A more detailed description of the procedure and example of raw data is found in ESI Section S5 and Fig. S4,† respectively.

# Results

### Reactor characterization – $O_3$ surface removal and comparison with literature

We found that $v_{dO_3}$ and $\gamma_{O_3}$ on clean glass increased with RH, decreased with increasing $O_3$ exposure time and ranged from 0.010–0.058 cm $s^{-1}$ and 1.1–6.5 ($\times 10^{-6}$), respectively (Table 1). These values were consistent with measurements and predictions reported in the literature.[60,83,84] The effect of surface aging that caused $O_3$ deposition to slow with exposure time and the increased $O_3$ removal with increasing RH have been observed for many indoor materials.[60,85] The smallest measured values reported in literature and summarized in Table 1 were derived from experiments after surfaces were aged for several hours. Our results were obtained on fresh glass surfaces and agreed most closely with results that also observed removal under short-term exposure.[83] Overall, agreement with literature values for $v_{dO_3}$ and $\gamma_{O_3}$ (Table 1) provided confidence in the use of this flow reactor design for the study of gas surface removal by indoor materials. The normalized $O_3$ concentration $\ln(C_i/C_0)$ *vs.* sampling position for clean glass under dry, mid, and high RH conditions from which $k_{wall}$ was derived are reported in Fig. S5.†

### Transport-limited deposition velocity for $O_3$ and 1,2-ISOPOOH

As shown in Fig. S5,† $O_3$ removal to clean glass fell between removal by halocarbon wax (minimum reaction-limited uptake constraint) and KI (maximum transport-limited uptake constraint). The smallest deposition velocity was observed on halocarbon wax at 0.006 cm $s^{-1}$ and 0.008 cm $s^{-1}$ when dry (10% RH) and humid (90% RH), respectively. As expected, the largest $O_3$ removal was observed on KI coatings, which yielded a $v_{tO_3}$ of 0.161 cm $s^{-1}$. Following standard practice,[76–78] the experimentally determined $v_{tO_3}$ was then used to estimate the transport-limited deposition for a different gas, which in this case is for 1-2-ISOPOOH, in our system. Based on the ratio of $O_3$ and 1,2-ISOPOOH diffusivities to the 2/3 power, the transport-limited deposition velocity of 1,2-ISOPOOH ($v_{ti}$) was estimated to be 0.74 times $v_{tO_3}$. Specifically, a $v_{ti}$ of 0.119 cm $s^{-1}$ was determined (see ESI Section S7†).

### Surface film characterization

Authentically-soiled glass surfaces held hygroscopic species, which can be expected to facilitate water uptake and sorption of water-soluble ROOHs at higher RHs (Fig. 2). Glass soiled in House C had the lowest mass loading of most components. However, variations in measured surface constituents across homes were modest. Briefly, we found that the major components were total WSOC (941–1229 ng-C $cm^{-2}$), acetate (158–257 ng $cm^{-2}$), chloride ($Cl^-$; 342–625 ng $cm^{-2}$), sulfate ($SO_4^{2-}$; 274–348 ng $cm^{-2}$), and water (434–481 ng $cm^{-2}$). On a carbon basis, 74–140 ng-C $cm^{-2}$ of the total WSOC (8–12%) came from acetate, formate, and oxalate (combined), where the remaining organic carbon fraction was uncharacterized. AFM-IR showed the presence of deposited particles (~50–100 nm) and a ~50 nm discontinuous organic film on the glass (ESI Section S8 and Fig. S6†). Surfaces were spatially heterogeneous, both physically and chemically, and carbonyl functional groups were more prominently observed in the deposited particles (Fig. S6†).

### 1,2-ISOPOOH uptake to clean and authentically soiled glass

1,2-ISOPOOH uptake on soiled glass was greater than clean glass and, like ozone, uptake increased with RH and decreased with increasing exposure time (Fig. 3). A reduction in 1,2-ISOPOOH uptake rates with exposure time would be expected whether 1,2-ISOPOOH was sorbing to surface sites to reach equilibrium partitioning as is known to occur for semi-volatile organic compounds[20] or undergoing heterogeneous reactions passivating the surface as is known to occur for $O_3$.[60] The system was not sensitive enough to determine if the conditions were at steady-state after removal was no longer observable.

Humidity, presumably through adsorbed and/or absorbed water, had a dramatic effect on 1,2-ISOPOOH uptake to soiled glass, especially at high RH (Fig. 3a–c and S7a–c†). In contrast,

Table 1 Deposition velocities ($v_{dO_3}$) and reaction probabilities ($\gamma_{O_3}$) for $O_3$ on clean glass under high, mid, and dry RH[a]

| Reference | Material | RH | Exposure time | $V_{dO_3}$ (cm $s^{-1}$) | $\gamma_{O_3}$ ($\times 10^{-6}$) |
|---|---|---|---|---|---|
| This work | Glass | 94% | Short (8 min; 40 min) | 0.058; 0.028 | 6.5; 3.1 |
| | | 54% | | 0.035; 0.014 | 3.9; 1.6 |
| | | 2% | | 0.027; 0.010 | 3.0; 1.1 |
| Cano-Ruiz *et al.*(1993)[60] [b] | Glass, aluminum | | Prolonged (typically hours) | | 6–0.06 |
| | Latex paint, brick, concrete | | | | 200–3 |
| Grøntoft & Raychaudhuri (2004)[84] | Glass | 90% | Prolonged (48 hours) | 0.00025 | |
| | | 50% | | 0.00015 | |
| | | 0% | | 0.0001 | |
| Gall & Rim (2018)[83] | Glass | 49% | Short (0–2 hours) | 0.020–0.002 | 0.74–0.06 |
| | Soiled glass[c] | 49% | Short (0–2 hours) | 0.025–0.002 | 1.2–0.15 |

[a] Values given for this work are uptake parameters at 8 and 40 minutes of $O_3$ exposure. Deposition velocities and reaction probabilities for $O_3$ and glass, soiled glass and a few other materials from literature are also reported. [b] Cano-Ruiz *et al.* (1993)[60] summarized reported and calculated values from literature. [c] Gall and Rim (2018)[83] reported measured values where glass plates soiled in a residence or office for up to 56 days were exposed to ozone in chamber experiments.

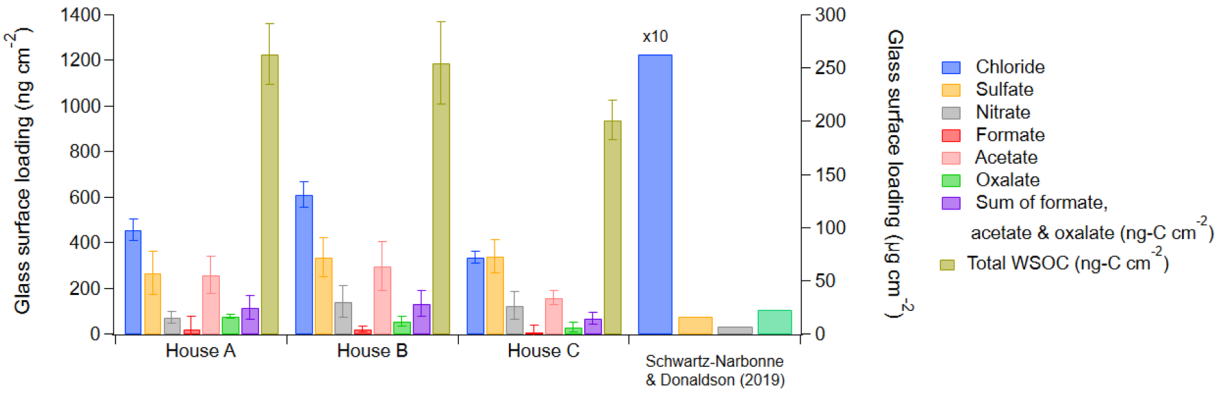


Fig. 2 Surface loadings of anions and water-soluble organic carbon (WSOC, on carbon basis) on authentically-soiled glass slides. The mass loading of species from House A–C are plotted on the primary $y$-axis. Average blank-corrected anion mass per surface area (mean ± $\sigma$; in ng cm$^{-2}$) from Houses A–C were as follows: chloride: 476 (142), sulfate: 323 (42), nitrate: 120 (36), formate: 25 (8), acetate: 244 (72), and oxalate: 61 (24). Surface loadings of anions on glass surfaces authentically soiled in a living room in a Toronto home from the Schwartz-Nabonne & Donaldson study were orders of magnitude larger and are shown for comparison on the secondary $y$-axis in units of µg cm$^{-2}$.[22]

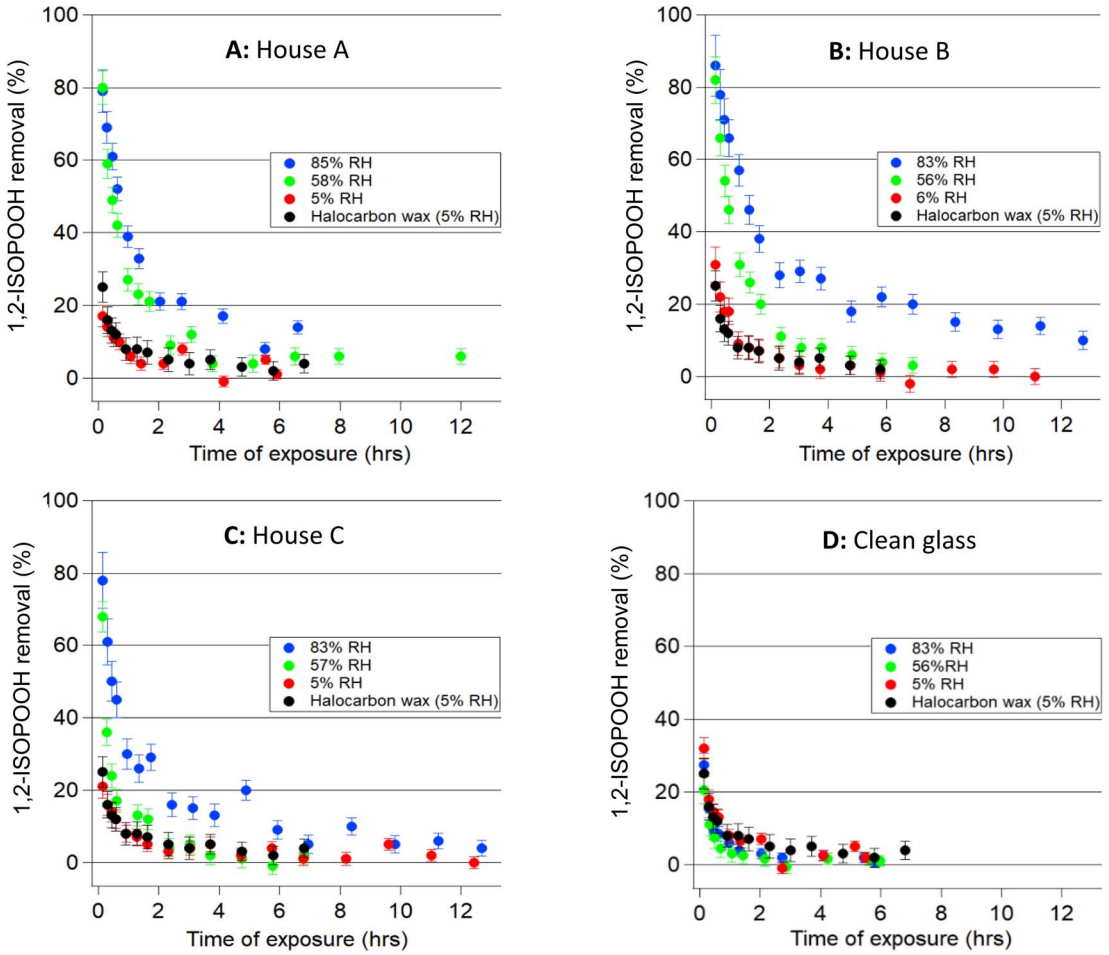


Fig. 3 Percent of 1,2-ISOPOOH removed by surface uptake as a function of exposure time for clean and authentically soiled glass, respectively. (A) House A glass. (B) House B glass. (C) House C glass (D) Clean glass. Shown are low RH (red markers), mid RH (green markers), and high RH (blue markers) conditions, as well as percent removal by halocarbon wax coated glass at low RH (black markers). Removal by soiled glass and clean glass was measured at $x_{93}$ (surface area for uptake: 0.19 m$^2$) and $x_{78}$ (surface area for uptake: 0.16 m$^2$), respectively. Error bars represent the normalized standard deviation of the 1,2-ISOPOOH signal at steady state.

 

removal by clean glass was insensitive to RH and minimal across the RH range (Fig. 3d and S7d†). Enhanced removal to soiled glass at high RH was sustained for >12 hours. Under mid RH conditions, enhanced removal relative to the dry RH conditions was only clearly observable for 2–4 hours. Under dry RH conditions (5–6% RH), there was no significant enhancement of 1,2-ISOPOOH removal by soiled glass compared to clean glass. Percent removal by clean glass across the RH range, soiled glass under dry (5% RH) conditions and halocarbon wax were minimal and not significantly different. The substantial increase in 1,2-ISOPOOH removal with increasing RH on soiled glass suggests that more humid conditions favor ROOH deposition in real homes, which may reduce ROOH inhalation exposures. However, the additional impacts of ROOH surface removal in humid homes on air quality depend on the fate (including possible chemical transformations) of the deposited ROOHs.

Cumulative molar uptake of 1,2-ISOPOOH on soiled glass (nmol $cm^{-2}$) increased with RH, ranging from 0.1–0.3, 0.2–0.5, and 0.5–0.9 nmol $cm^{-2}$ (across homes) under dry, mid and high RH conditions, respectively, after 6 hours of exposure (Fig. 4). The cumulative molar uptake of 1,2-ISOPOOH to glass surfaces after 6 hours was estimated by integrating the uptake over time at each RH. Molar uptake of 1,2-ISOPOOH ranged between 0.1 and 0.9 nmol $cm^{-2}$ on soiled glass and 0.1–0.3 nmol $cm^{-2}$ on clean glass across the RH range. Under high RH, only glass soiled in Houses B and C were exposed to 1,2-ISOPOOH for >6 hours. After 12 hours of exposure under high RH (Fig. S8†), the molar uptake nearly doubled from 0.9 to 1.6 nmol $cm^{-2}$ for House B and from 0.5 to 0.8 nmol $cm^{-2}$ for House C. Note the reported molar uptake does not consider the fate of 1,2-ISOPOOH once adsorbed, but only the total moles of 1,2-ISOPOOH that deposited per $cm^2$.

1,2-ISOPOOH uptake to glass soiled in House C was smaller than that to glass soiled in the House A and B. Note that glass from House C was less soiled than glass from House A and B (Fig. 2). House C surface films contained lower quantities of hygroscopic chloride and WSOC, which may have reduced its loading of surface-associated water relative to the other 2 homes. Less mass accretion on glass could mean a larger fraction of the glass surface area was unsoiled and resembled clean glass, ultimately reducing the RH enhancement of ROOH deposition. Compositional differences in the organic fraction of surface films that may result in different chemical and physical properties could also be a factor that influenced ISOPOOH removal to surfaces from each home, especially if there were different quantities of species reactive toward peroxides (see insights into chemistry in Discussion: Potential surface chemistry). Under dry RH, cleaner glass surfaces (clean and House C glass) seemed to have had a higher capacity for 1,2-ISOPOOH uptake than dirtier surfaces (House A and B glass). Unlike Houses A and B, the molar uptake at low RH for House C and clean glass was slightly higher than the molar uptake at mid RH. On clean glass, this may suggest competition between 1,2-ISOPOOH and water molecules for adsorption sites under mid RH conditions and that 1,2-ISOPOOH was free to occupy all adsorption sites under dry RH conditions. At high RH, perhaps a damper surface provides a larger water film for 1,2-ISOPOOH uptake, compensating for water occupation of adsorption sites. On glass soiled in House C, this could suggest less surface coverage of indoor grime and more exposed clean glass surface area than glass soiled in Houses A and B. This could suggest that the dominant physical and chemical pathways in the ISOPOOH uptake mechanism could be different for relatively clean surfaces compared to heavily soiled glass. Alternatively, it is possible that we have not fully accounted for uncertainties in the I-HR-TOF-CIMS calibration and the differences between mid-RH and dry conditions for House C and clean glass are, in reality, not significant. I-HR-TOF-CIMS calibration did not affect the other types of calculations in this paper because they use the normalized signal.

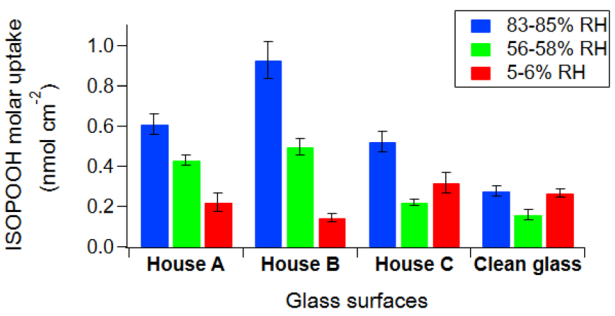


Fig. 4 The cumulative molar uptake of 1,2-ISOPOOH (nmol $cm^{-2}$) on clean glass and glass soiled in Houses A, B and C after 6 hours of exposure. Error bars were propagated from percent removal plots.

### Deposition velocity of 1,2-ISOPOOH ($v_{di}$)

Fig. 5 compares $v_{di}$ for clean glass and glass soiled in each home at each RH. 1,2-ISOPOOH deposition velocity fell between the $v_{di}$ observed on halocarbon wax and that estimated for transport-limited uptake conditions (Fig. S7†), but $v_{di}$ on soiled surfaces when dry and to clean glass at each RH was similar to removal by halocarbon wax. The initial $v_{di}$ approached transport-limited conditions likely due to the surface being "fresh" with respect to 1,2-ISOPOOH and less resistant to uptake. The average $v_{di}$ to halocarbon wax after removal was no longer observable (~2 hours of exposure) provided a limit of quantification (LOQ) for $v_d$ of 0.001 cm $s^{-1}$. The RH dependence of the initial normalized 1,2-ISOPOOH signal at location $x_i$ ($\ln C_i/C_0$) *vs.* sampling position for glass soiled in Houses A, B, C and clean and halocarbon wax coated glass from which $k_{wall}$ is derived is reported in ESI (Fig. S7†).

Humidity induced a large increase in initial $v_{di}$ (8 min of exposure) on soiled glass across homes, with a $v_{di}$ that ranged from 0.04–0.06 cm $s^{-1}$ at high RH, 0.03–0.05 cm $s^{-1}$ at mid RH, and 0.004–0.02 at dry RH. The same humidity effect was not observed on clean glass where $v_{di}$ was only 0.013, 0.009 and 0.016 cm $s^{-1}$ at high, mid, and dry RH, respectively. From 16 min to 1 hour of exposure, an order of magnitude enhancement in $v_{di}$ (0.01 *vs.* 0.001 cm $s^{-1}$) to soiled glass, relative to clean glass, was sustained under high RH. A substantially larger $v_{di}$ at 83–85% RH and 56–58% RH (Fig. 5A

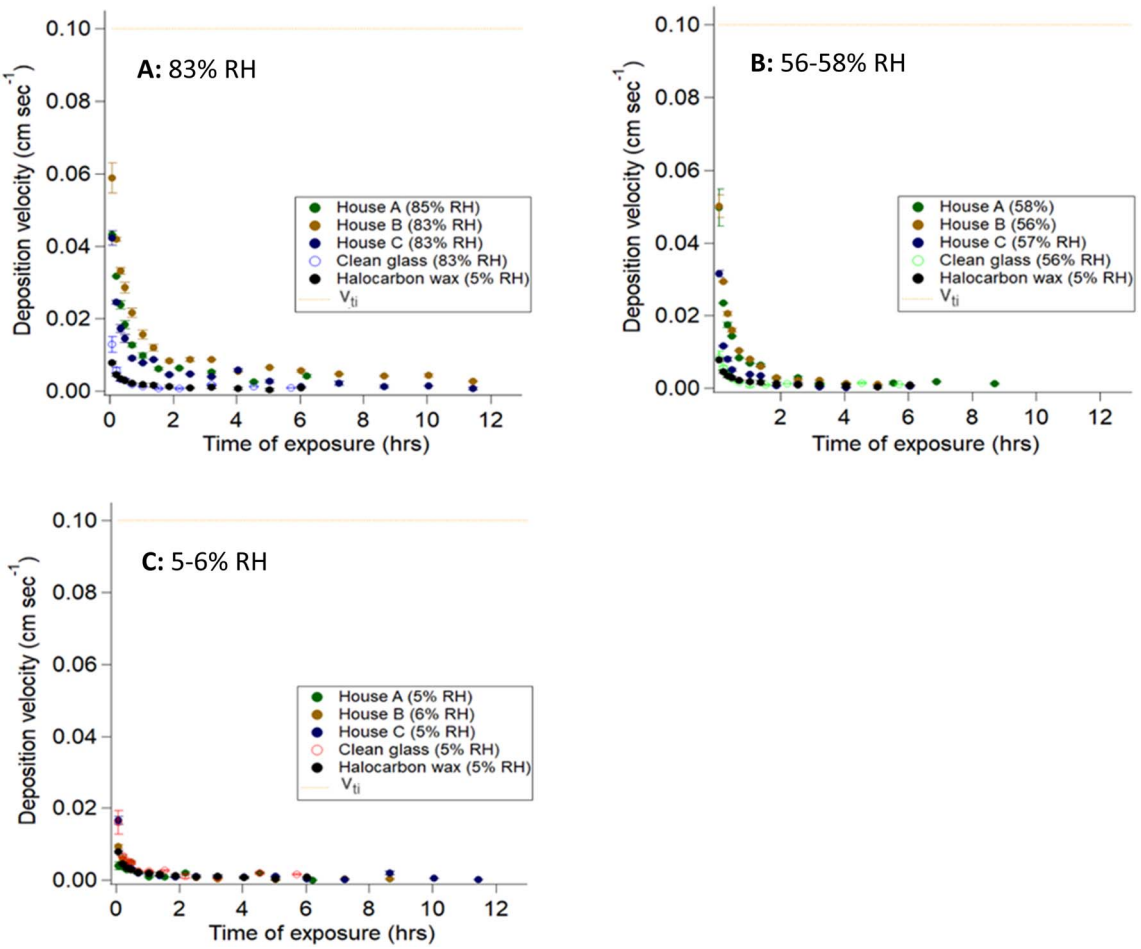


Fig. 5 1,2-ISOPOOH deposition velocity on clean and soiled glass at each RH and on halocarbon wax coated glass at low RH. (A) $v_{di}$, high RH (B) $v_{di}$, mid RH (C) $v_{di}$, low RH. The $v_{ti}$ is displayed (gold dotted line) to show how close initial $v_{di}$ comes to the transport-limited removal rate. Error bars were extrapolated from the standard deviation in $k_{wall}$ (Fig. S7†).

and B) than 5–6% RH (Fig. 5C) for soiled glass was sustained for hours. This enhancement was sustained for >12 hours under high RH and 4 hours under mid RH until the LOQ ($v_{di}$ = 0.001 cm $s^{-1}$) was reached. The time to LOQ in the system is denoted as $\tau_{LOQ}$. This suggests a lower quantity of adsorbed water or reactive aqueous sites on clean glass when humid than on humidified soiled glass. Compared to Houses A and B, glass soiled in House C was the most resistant to 1,2-ISOPOOH uptake when humid, especially at mid RH. Under dry conditions, the $v_{di}$ of soiled glass was not significantly greater than that of clean glass (Fig. 5C), emphasizing the importance of surface soiling on the observed humidity effect. At 55–56% RH, as exposure time increased, $v_{di}$ decreased. This resulted in values ranging from 0.050 cm $s^{-1}$ (upper bound, fresh surface) to 0.001 cm $s^{-1}$ (lower bound, aged surface) at a home relevant 56–58% RH.

### Reaction probability of 1,2-ISOPOOH

Reaction probabilities, deposition velocities and $\tau_{LOQ}$ for all scenarios are reported in Table 2. Like $\gamma_{O_3}$, a range was reported for $\gamma_i$ due to observed surface aging. Reaction probability and $\tau_{LOQ}$ increased with RH on soiled glass but not clean glass. The $\gamma_i$ ranged from 0.1–4.6 ($\times 10^{-6}$) across glass surfaces, RH and exposure time. Initial reaction probabilities ranged from 0.4–0.6 ($\times 10^{-6}$), 1.3–3.2 ($\times 10^{-6}$), and 2.7–4.6 ($\times 10^{-6}$) for soiled glass across homes under dry, mid and high RH, respectively. A smaller range of initial reaction probabilities were observed on clean glass across RHs from 0.6–0.8 ($\times 10^{-6}$). Reaction probabilities were highest for glass soiled in House B followed by House A then C. The initial $\gamma_i$ and $\tau_{LOQ}$ at mid and high RH was largest on house B glass at each RH, followed by house A, house C and then clean glass. (House C and clean glass showed the highest initial reaction probabilities at dry RH).

Generally, $\gamma$ is limited to describing only irreversible reactive uptake of gases. While the measurements do not definitively show that irreversible reactive uptake occurs, the characteristic time, $\tau_{SS}$ to steady state (ESI Section S10†) suggests uptake solely due to partitioning with an organic or aqueous film should be on the order of only a few minutes (<3 minutes), supporting the case for reactive uptake; note our measurements approached steady state, however, actual time to steady-state in the system remains uncertain due to sensitivity limitations when uptake rates became too small to measure. The $\tau_{LOQ}$ were much longer

 

Table 2 1,2-ISOPOOH reaction probability ($\gamma_i$) and deposition velocity ($v_{di}$) at 8 minutes of exposure and at the time it reaches the limit of quantitation ($\tau_{LOQ}$)[a]

| | 5–6% RH | | | 56–58% RH | | | 83–85% RH | | |
|---|---|---|---|---|---|---|---|---|---|
| Glass surface | $v_{di}$ (cm s$^{-1}$) @ 8 min; $\tau_{LOQ}$ | $\gamma_i$ ($10^{-6}$) @ 8 min; $\tau_{LOQ}$ | $\tau_{LOQ}$ (h) | $v_{di}$ (cm s$^{-1}$) @ 8 min; $\tau_{LOQ}$ | $\gamma_i$ ($10^{-6}$) @8 min; $\tau_{LOQ}$ | $\tau_{LOQ}$ (hr) | $v_{di}$ (cm s$^{-1}$) @ 8 min; $\tau_{LOQ}$ | $\gamma_i$ ($10^{-6}$) @ 8 min; $\tau_{LOQ}$ | $\tau_{LOQ}$ (h) |
| House A | 0.004; 0.001 [0.001; 0.0001] | 0.4; 0.1 [0.01; 0.01] | 1 | 0.050; 0.001 [0.005; 0.0002] | 2.6; 0.14 [0.02; 0.03] | 3 | 0.043; 0.004 [0.0001; 0.0003] | 3.5; 0.5 [0.01; 0.04] | >6 |
| House B | 0.009; 0.001 [0.0006; 0.0001] | 0.6; 0.1 [0.04; 0.04] | 2 | 0.050; 0.001 [0.003; 0.0001] | 3.2; 0.15 [0.02; 0.04] | 4 | 0.059; 0.003 [0.004; 0.0002] | 4.6; 0.3 [0.09; 0.02] | >12 |
| House C | 0.017; 0.001 [0.001; 0.0003] | 0.5; 0.1 [0.03; 0.01] | 1 | 0.031; 0.001 [0.001; 0.0001] | 1.3; 0.12 [0.02; 0.03] | 2 | 0.042; 0.001 [0.002; 0.0003] | 2.7; 0.2 [0.04; 0.01] | 6 |
| Clean | 0.016; 0.001 [0.003; 0.0002] | 0.8; 0.1 [0.05; 0.05] | 1 | 0.009; 0.001 [0.002; 0.0001] | 0.6; 0.1 [0.05; 0.06] | 1 | 0.013; 0.001 [0.002; 0.0001] | 0.6; 0.1 [0.08; 0.01] | 1 |

[a] Errors (in parentheses) were extrapolated from the standard deviation in the wall loss rate coefficient ($k_{wall}$). Under high RH, neither glass soiled in House A or House B was sufficiently exposed to 1,2-ISOPOOH to reach steady state, so time to steady state was listed as greater than 6 or 12 hours; a $v_{di}$ of 0.004 cm s$^{-1}$ and 0.003 cm s$^{-1}$ was achieved after 6 hours of exposure for House A glass and 12 hours of exposure for House B glass, respectively. Uncertainties for initial and later results are shown in brackets.

than the estimated $\tau_{SS}$. The continued 1,2-ISOPOOH uptake substantially beyond the $\tau_{SS}$ on soiled glass under mid and high RH suggests that 1,2-ISOPOOH undergoes reactive uptake on soiled glass in the presence of humid conditions, especially at high RH where uptake was sustained for several hours beyond what was observed on clean glass. Under dry conditions, the $\tau_{LOQ}$ (1 h) was the same for soiled and clean glass except for glass soiled in House B (2 h). This suggests that chemistry, or at least more chemistry, was enabled by the assumed presence of adsorbed water on soiled glass when humid.

# Discussion

### Comparisons and insight from other studies

To our knowledge, these are the first direct measurements of the deposition velocity of an ROOH to naturally soiled indoor window surfaces. Because of a lack of measurements, hydrogen peroxide, being a reactive gas, was assumed to deposit on surfaces near the transport-limited rate in early indoor models.[87] Since then, models have continued to use an estimated $v_d$ of 0.07 cm s$^{-1}$ for hydrogen peroxide[63] and organic peroxides.[63] The initial $v_{di}$ to soiled glass under humid conditions when the glass surfaces were fresh with respect to ROOH exposure (0.03–0.06 cm s$^{-1}$ across homes after 8 minutes of exposure), are relatively close but smaller than the estimated ROOH $v_d$ from literature, recognizing that the later number includes not only glass, but also painted walls and carpets, which should have higher $v_{di}$ than smooth impermeable surfaces. Since most sorptive uptake is predicted to occur within just a few minutes (ESI Section S10†), we believe the initial values shown in Table 2 (8 minutes values) are most representative of the reactivity of the authentically soiled glass when it was removed from the homes. These initial values may best capture ROOH uptake to typical surfaces that are in continual balance of aging and replenishment, like we expect the soiled glass was when it was loaded into the reactor and removed from the homes. The range of the initial $v_{di}$ (0.03–0.06 cm s$^{-1}$) measured here supports the use of values in this range to model uptake of organic peroxides.

Under home-relevant mid RH conditions, our experimentally determined $v_{di}$ after 1,2-ISOPOOH exposures of ~1 hour (0.007 cm s$^{-1}$ across homes, on average) is much lower than the initial values. Later values represent the changing reactive nature of an aging surface film that is being quenched/oxidized by ISOPOOH at a relatively high mixing ratio of up to 300 ppb. Real surface films replenish with depositing gases and particles from contact with room air, and as a result, may not ever be completely fresh or aged.[88] The average $v_{di}$ (0.010 cm s$^{-1}$) observed under humid conditions is likely too low for typical indoor conditions. However, it could represent a conservative value for ROOH deposition in indoor models for a surface that may be more heavily aged; for example, this could be aging from consecutive cleaning activities that release spikes of ROOH or from competitive film oxidation by other indoor oxidants.

Conveniently, surface–air partitioning coefficients for phthalates on impervious metal, glass and acrylic surfaces soiled with kitchen grime were independent of the type of

surface material, suggesting that the same uptake kinetics can apply to all similarly soiled impermeable smooth surfaces in a residence,[90] or at least in the same room (*e.g.*, kitchen or bathroom).[21,22] Therefore, the deposition velocities reported here may be applied to modeling surface removal to all vertical impermeable surfaces in each residence, especially in the main living area; values can also be considered a lower bound for ROOH $v_d$ to horizontal surfaces that likely contained more accreted mass from settled particles. Although wider home-to-home variation in $v_d$ may have been observed if more homes were studied, the reported data provide valuable model inputs that were derived on authentic surface films under realistic RH conditions that could be reasonably used in comprehensive models.

Water was also expected to sorb to both clean and soiled glass. Deposited particles and organic films containing polar functional groups and inorganic ions should provide more hygroscopic surface area for water to adsorb/absorb than a flat clean glass surface (*i.e.*, silicate groups). Surface water content was not measured in this work. It should be noted that Or *et al.* observed evidence of hygroscopic growth on indoor films and deposited particles on authentically-soiled glass surfaces using AFM-IR[29] and Schwartz-Narbonne & Donaldson measured roughly 0.4 μg $cm^{-2}$ water uptake on authentically-soiled quartz crystals at 50% RH using a quartz crystal microbalance.[22] Furthermore, water uptake has been shown to decrease secondary organic aerosol viscosity and, as a result, increase uptake and diffusion of water-soluble species in aqueous-organic aerosols.[71] We expect water uptake occurred to soiled glass under humid conditions, changing surface film properties and aiding 1,2-ISOPOOH uptake. Although even a dry, oily and viscous film should increase the surface area compared to clean flat glass, the authentic film did not enhance 1,2-ISOPOOH removal at 5% RH compared to clean glass, suggesting enhancement of ROOH uptake by the dry film was either too small to differentiate from clean glass or the dry film was similarly resistant to uptake as clean glass. If the clean glass was indeed perfectly clean and no reactive uptake occurred (assuming no decomposition at the clean glass interface), then the 1 hour $\tau_{LOQ}$ showed the duration of exposure needed for 1,2-ISOPOOH to reach sorptive equilibrium with both the glass surfaces and any sorbed water. The $\tau_{LOQ}$ on soiled glass under humid conditions was 2 to at least 6 times longer than under dry conditions and 2 to at least 12 times longer than on clean glass under all RH conditions.

Similarly, Gall and Rim[83] determined $O_3$ surface removal by clean glass was only observable for 2 hours, while $O_3$ uptake to soiled glass was observable up to 4 hours at 49% RH. Furthermore, their molar uptake of $O_3$ increased on soiled glass surfaces containing higher quantities of accreted mass with the molar uptake of $O_3$ ranging from 0.1–0.4 nmol $cm^{-2}$.[83] In our work, glass soiled in House B had the most accreted mass of measured species, and the $\tau_{LOQ}$ was twice as long as other samples, suggesting higher mass accretion could have played a role. Although ROOH and $O_3$ surface chemistry would undergo different mechanisms, we observed a similar magnitude of 1,2-ISOPOOH molar uptake to soiled glass in this study, and modest evidence that lower mass accretion of hygroscopic species may have reduced the RH enhancement of peroxide uptake to glass soiled in House C and clean glass.

To assess the observed mass accretion on soiled glass, the surface loadings of hygroscopic species were compared to previous studies. The concentrations of total WSOC were in the range of those reported by other groups that extracted polar organic compounds from indoor window surfaces,[91,92] but anion concentrations were much smaller than those reported by Schwartz-Narbonne and Donaldson (see Fig. 2).[22] Schwartz-Narbonne and Donaldson deployed horizontal glass substrates (glass soda-lime glass beads single layered in Petri dishes)[22] that should collect more settling coarse particles[20] than the glass slides in this study which were mounted vertically. This could, in part, explain the differences in order of magnitude (both studies extracted glass substrates in water). Ultimately, surface loadings of 1,2-ISOPOOH may be expected to increase with accreted masses of hygroscopic species and water on soiled surfaces under humid conditions. Of course, the composition of the surface films may affect the potential fate (including possible chemical transformations) of 1,2-ISOPOOH once taken up by the surface.

### Potential surface chemistry

The products, mechanisms and kinetics of aqueous multiphase indoor ROOH chemistry are not well understood, but the aerosol literature provides some insights. ROOHs in indoor surface-associated water could hydrolyze[93] or act directly as an oxidant,[86,94] releasing carbonyl compounds (*e.g.*, carboxylic acids or aldehydes)[55,95,96] and $H_2O_2$;[53,55,96] its decomposition could also generate radicals as has been demonstrated for wet aerosols.[97–99] Further, radical formation could drive oxidation of surface-bound organic compounds.[97,100,101] ROOH has been shown to drive multiphase formation of organosulfates in the presence of water and acidity,[47] and participate in other accretion reactions forming oligomeric compounds.[54,102]

ROOHs can decompose in water to generate hydroxyl (OH) and organic radicals (RO) that could further oxidatively age deposited particles and surface films.[97,103] Tong *et al.* observed significant OH radical formation when filter-extracted SOA (formed from terpene ozonolysis) interacted with liquid water under dark conditions and in the absence of iron metals (Fenton chemistry);[97] addition of $Fe^{2+}$ to the aqueous SOA extracts increased molar OH yield 15-fold.[97] They concluded that their observations provided evidence of ROOH hydrolysis and thermal decomposition into radicals.[97] Such multiphase chemistry could be relevant to indoor conditions where photolysis rates are expected to be lower[104] and the concentration of metals is likely smaller than outdoors based on measurements of indoor and outdoor dust.[105,106] Furthermore, the thermolysis pathway to decomposition into radicals in aerosols has been shown to occur at room temperature.[107,108] Fenton-like reactions of $H_2O_2$ (ref. 109) and ROOHs[99] with iron metal ions (*e.g.*, $Fe^{2+}$ and $Fe^{3+}$) are another route to OH or both OH and RO production in the aqueous phase, respectively;[110] 1,2-ISOPOOH can undergo Fenton-like reactions catalyzed by

 

transition metals in the aqueous phase leading to either homolytic cleavage releasing alkoxy radicals that decompose into methyl vinyl ketone (MVK) and formaldehyde,[41] or heterolytic cleavage releasing OH and alkoxyl radicals,[99] but this may be hindered by the presence of chloride ions as seen for Fenton-like decomposition of $H_2O_2$ in aqueous solution.[111] Little is known about the abundance of transition metals such as iron in indoor surface films, however their indoor surface concentrations could be considerably lower, on average, than in outdoor aerosol. Transition metals can be found in paint[112] and are transported in from outdoor soil and in aerosol of outdoor origin, particularly coarse aerosol.[113] Indoor-to-outdoor ratios of metals in dust are generally <1.[105,106] Radicals from 1,2-ISOPOOH chemistry could initiate chemistry with other surface constituents with possible implications such as consumption of adsorbed alkenes, and thus, secondary generation of ROs in the surface film that may propagate further chemistry, depending on the products that formed.[114] Small water-soluble gases (*e.g.*, acetic acid), for example, could undergo multiphase chemistry in the presence of such OH radicals in aqueous surface films, ultimately forming semi- and low-volatility products (*e.g.*, organic acids and oligomers).[114,115]

ROOHs have also been shown to hydrolyze in aqueous aerosols and form carbonyl compounds and $H_2O_2$;[93] this is enabled by the presence of water[116] and catalyzed by acids.[96] For example, ROOHs generated from the ozonolysis of terpenes have been shown to readily decompose into aldehydes and $H_2O_2$ on acidified aerosols,[96] including when acidified with small organic acids, which are ubiquitous species indoors.[30,58] Aerosol water and acidity have been shown to promote reactive uptake of ISOPOOH.[53,55,56,95] A major fate of 1,2-ISOPOOH in acidified sulfate aerosols is acidic cleavage of the O–O bond leading to gas-phase decomposition products (hydroxy acetone and acetaldehyde).[95] These products were not detected in the gases leaving the reactor in the current study, either because they were not produced or, more likely, because the I-HR-TOF-CIMS is not very sensitive to these small carbonyl compounds.[117]

Differences in acidity between soiled indoor surfaces and outdoor aerosol are likely and can be expected to influence the chemistry. Organic and inorganic acids, as well as bases, are ubiquitous indoors and known to have dynamic surface interactions,[58] especially with sorbed water.[18,31,118] Nazaroff & Weschler predicted that, in the absence of other acids and bases, indoor levels of basic $NH_3$ (15–75 ppb) and acidic $CO_2$ (500–1000 ppm) would maintain condensed water at a neutral pH (~7–7.5 pH under typical conditions).[58] However, organic acids may also influence pH. They are the most abundant class of WSOGs in indoor air;[30] they are polar organic compounds, can be expected to be present in indoor surface films,[24] and the partitioning of small carboxylic acids is already known to influence pH conditions of atmospheric aerosols.[57,119] As a result, indoor surface films are predicted to be neutral (pH ~ 7) to slightly acidic (pH < 7) from heterogenous acid–base chemistry, but surface pH is largely unknown.[58] Deposited particles could be key sites for acidic conditions on surfaces, although indoor conditions (*e.g.*, $NH_3$ levels) are expected to partially neutralize strong acidic aerosols transported in from outdoors,[58,120,121] where their pH is typically much lower (*e.g.*, 0.5–3 in the southeastern US).[57,122]

In this study (Fig. S6†) and others,[29,123] spectral images identified carbonyl and/or carboxylate functionalities (suggesting protonated and deprotonated forms) in deposited particles on soiled glass; these could be largely attributed to fatty acids from cooking emissions. Acid-catalyzed decomposition would not explain the observed surface aging, as the acid responsible for bond cleavage would be recycled and available for additional chemistry. Perhaps aqueous-mediated ROOH decomposition into volatile products dominates removal at near steady-state conditions, especially at high RH where removal was sustained for longer.

As in aerosols,[93,94,97,124] multiphase ROOH chemistry could directly oxidize reduced species present on indoor surfaces, altering both the composition of the indoor air and the indoor surfaces. Multiphase oxidation of sulfite by 1,2-ISOPOOH in aerosols is predicted to produce 3% of total aerosol phase sulfate in the southeastern US[37] and produces MVK, hydrated formaldehyde, hydroxymethanesulfonate (HMS), 2-methyl-3-butene-1,2-diol, and acetic acid with 30%, 30%, 22%, and 5% molar yields, respectively.[86] $SO_2$ ($K_H$: 1.3 mol $L^{-1}$ $atm^{-1}$)[32] is estimated to be around 6 ppb indoors in the absence of indoor sources (*i.e.*, kerosene space heaters) and to be taken up to surfaces with an inferred $v_d$ of 0.005 cm $s^{-1}$ where it can convert to bisulfite ($HSO_3^-$) in the presence of adsorbed water.[58] Hydrogen peroxide oxidation of sulfite in the aqueous phase is already very well-known.[125] Furthermore, methyl hydroperoxide, peroxyacetic acid,[126] *tert*-butyl hydroperoxide, cumene hydroperoxide, 2-butanone peroxide,[94] and limonene-$O_3$ derived peroxides[127] have also been shown to oxidize sulfite. Humid conditions facilitate $SO_2$ uptake to aerosols.[127] However, this chemistry is also pH dependent, with low aerosol pH increasing peroxide reaction rates with dissolved $SO_2$ in the aqueous phase.[94] The pH dependency of this chemistry was generally greater for $H_2O_2$ than organic peroxides.[86,94] Similarly, hydrogen peroxide has been shown to oxidize both nitrite in the presence of iron and nitrous acids into $NO_2$.[125] Because of the substantial contribution of organics on soiled indoor surfaces, it is worth also considering the potential for multiphase oxidation of organic species by ROOH in the indoor environment.

It is also possible that accretion reactions may be responsible, in part, for the observed surface aging due to consumption of reactants or low volatility products that change film properties such as a lowering of viscosity that can impede diffusion. Another peroxide chemical pathway in aerosols is ROOH nucleophilic addition with condensed aldehydes forming peroxyhemiacetals;[34,54,128] it is unclear if this chemistry would be reversible or not. Oxidation chemistry,[78,129] material off-gasing[130] and human activities[131] are sources of indoor aldehydes,[132] some of which are semi- and low-volatility and can partition or accumulate in indoor surface films,[21,29,131] where they could reasonably participate in reactive uptake of ROOHs. ROOHs can also react directly with Criegee intermediates from ozone chemistry, forming oligomeric ROOHs that should favor condensed phases.[102]

## Implications

As with $O_3$, deposition to surfaces may be an important sink that reduces ROOH concentrations in indoor air. Indoors, surface area-to-volume (S/V) ratios are orders of magnitude greater than outdoors.[58] A typical S/V ratio for a furnished room is 3 $m^{-1}$,[13,133] excluding microscopic surface area.[77] The average initial (after 8 minutes of exposure) $v_{di}$ for 1,2-ISOPOOH under humid conditions across homes was 0.05 cm $s^{-1}$ (or 1.6 m $h^{-1}$). Assuming this deposition velocity can be applied to all indoor surfaces, a given S/V ratio and average $v_d$ can be used to estimate a loss rate to surfaces ($k_s$):[87]

$$k_s = v_{di} S/V \quad (3)$$

Therefore, the loss rate of gaseous ROOH to surfaces in a typical room would be ~4.8 $h^{-1}$ (using the range of initial $v_{di}$, $k_s$ = ~3–6 $h^{-1}$) which is greater than the typical range of air changes per hour (0.2–2.0 ACH),[51,134] and mean residential ACH in large scale studies (0.76 ACH in 2844 US homes in a single study[5] or 0.5 ACH in 10 000 homes compiled from global data from different studies[135]); using the reported average $v_{di}$ (0.01 cm $s^{-1}$) across exposure times and observed under humid conditions, the surface removal rate would decrease to ~1 $h^{-1}$, which is competitive in scale with ventilation rates. A peroxide loss rate greater than typical ACH suggests surface removal would be an important loss mechanism for gas-phase ROOHs that may lower human inhalation exposure to peroxides. In contrast, the average $v_{di}$ and $k_s$ to clean glass was only 0.1 m $h^{-1}$ and 0.3 $h^{-1}$, respectively, indicating authentic surface films enhanced ROOH loss rates to glass surfaces by a factor of ~3.3 in the presence of humidity. Surface removal rates of ROOH by materials with higher intrinsic surface area (*e.g.*, fleecy or rough surfaces like paint) and surfaces that accumulate surface grime more rapidly (*e.g.*, floors), are likely to be higher.

Nazaroff *et al.*[61] calculated average indoor $O_3$ loss rates over all surfaces (including windows) from measurements in homes[136] or single bedrooms,[137] ranging from 0.05–1.2 $h^{-1}$. More recently, measurements of unperturbed $O_3$ dynamics in an occupied California residence yielded loss rates between 0.8-2 $h^{-1}$ with an overall best-fit of 1.3 $h^{-1}$.[138] This was on the low end of loss rates observed from perturbed indoor environments (*e.g.*, injecting $O_3$), which ranged between 1–8 $h^{-1}$ with an average of 2.8 $h^{-1}$ across 43 homes in California.[138,139] Duncan *et al.*[31] observed WSOG loss rates in the range of 0.2–2.2 $h^{-1}$ in a residence, with more oxygenated species decaying faster; no specific ROOHs were identified and the S/V ratio accounting for furnishing was not reported. $H_2O_2$ ($K_H$: 1.2 × $10^5$ mol $L^{-1}$ $atm^{-1}$)[39] decay rates after regular cleaning activities were recently measured in a test-chamber designed as a residential room and ranged from 8.5–37.1 $h^{-1}$, which was much higher than the room ventilation rate (0.51 $h^{-1}$) and increased with the S/V ratio of the room.[36] Zhou *et al.*[36] also observed a 1.8 $h^{-1}$ decay of $H_2O_2$ after a deep-cleaning perturbation, where peroxide cleaning solution was allowed to evaporate for a prolonged period. Furthermore, Zhou *et al.*[36] performed elevated ventilation experiments after which perturbed $H_2O_2$ mixing ratios did not rebound, strongly indicating that some surface removal was an irreversible process because of reactive uptake. Zhou *et al.*[36] postulated that $H_2O_2$ could have reacted with components in wood and paint (*e.g.*, titanium oxide in white wall paint)[140] in the model room. In a real indoor environment, reactions could also occur in surface films and other materials (*e.g.*, furnishing or carpets).

Overall, loss rates suggest ROOH concentrations indoors should be highly regulated by indoor surface dynamics. In the present study, ROOH irreversible removal would have to be from chemistry in surface films on humidified soiled glass or in residual films on cleaned glass. In addition to published estimates for ROOH decay rates indoors, dynamics reported here should be considered as inputs for the dynamics of ROOHs in indoor models.

## Limitations

In this work, 1,2-ISOPOOH was used as a model indoor ROOH to represent the dynamics of this class of indoor pollutants with real indoor surfaces. Like outdoors,[56,93,141–144] there is likely a plethora of ROOH compounds present indoors, due particularly to oxidation of indoor terpenes (*e.g.*, from air fresheners, cleaning products, wood materials)[145,146] but also from polycyclic aromatic hydrocarbons (*e.g.*, from pest repellant, deodorant, cooking)[147,148] and a variety of other potential sources.[93] Indoor surfaces should be a key site for the generation and consumption of ROOHs derived from heterogeneous chemistry of $O_3$ (ref. 89) and OH[149] with sorbed organics and consumption of ROOHs derived from gas-phase oxidation.[146] However, indoor ROOH is largely uncharacterized at the molecular level. Thus, the appropriateness of 1,2-ISOPOOH to represent the properties and behavior of all ROOH is not guaranteed.

In real homes, additional factors will also influence the fate of surface-associated peroxides. For example, real windows are exposed to sunlight during the day and loss of surface-associated organic peroxides *via* photolysis and photooxidation is plausible. While plausible, Zhou *et al.*[36] concluded that, unlike outdoors, photolysis and photooxidation of $H_2O_2$ is small to negligible indoors, estimating that these processes account for 0% and 0.3% of indoor $H_2O_2$ losses, respectively. Unlike in our experiments, indoor environments experience dynamic variations in concentrations of semi-volatile acids and bases that influence surface acidity and therefore surface chemistry.[58] Additionally, rough, fleecy or porous surfaces (*e.g.*, carpets and painted drywall) are found indoors and can be expected to have a larger deposition velocities than to soiled glass.[76] Also, permeable materials such as painted drywall are expected to have higher moisture contents at a given RH than window surfaces.[58] This may increase capacity for sorptive partitioning of water-soluble gases but could also dilute surface film acidity, affecting reaction pathways.[70]

The uptake dynamics reported herein changed with ROOH exposure times, from 8 minutes to hours of exposure for soiled surfaces. Thus, there is some uncertainty concerning the most appropriate values to use when modeling. As discussed, we recommend the use of initial values ($v_{di}$: 0.03–0.06 cm $s^{-1}$) for

 

modeling applications. Furthermore, the reported parameters are most applicable to vertical and smooth impermeable surfaces in the living or dining areas of residences, as they may be soiled more similarly to the glass used in this study.

## Conflicts of interest

The authors declare no conflicts of interest.

## Acknowledgements

This research was supported by the National Institute for Occupational Safety and Health (T42-OH008673) and the Alfred P. Sloan Foundation (G-2017-9794; G-2020-13937). We thank Glenn Walters, Professor of Practice in the Department of Applied Physical Sciences at the University of North Carolina at Chapel Hill, for manufacturing the novel flow reactor. We thank all study participants for allowing us to deploy glass samples in their homes.

## References

1 S. Batterman, F. C. Su, S. Li, B. Mukherjee, C. Jia and HEI Health Review Committee, Personal exposure to mixtures of volatile organic compounds: modeling and further analysis of the RIOPA data, *Res. Rep.–Health Eff. Inst.*, 2014, **2015**, 3–63.

2 L. A. Wallace, Personal exposure to 25 volatile organic compounds. EPA's 1987 team study in Los Angeles, California, *Toxicol. Ind. Health*, 1991, **7**, 203–208.

3 N. E. Klepeis, W. C. Nelson, W. R. Ott, J. P. Robinson, A. M. Tsang, P. Switzer, J. V. Behar, S. C. Hern and W. H. Engelmann, The National Human Activity Pattern Survey (NHAPS): a resource for assessing exposure to environmental pollutants, *J. Exposure Anal. Environ. Epidemiol.*, 2001, **11**, 231–252.

4 N. Yamamoto, D. G. Shendell, A. M. Winer and J. Zhang, Residential air exchange rates in three major US metropolitan areas: results from the Relationship Among Indoor, Outdoor, and Personal Air Study 1999-2001, *Indoor Air*, 2010, **20**, 85–90.

5 D. M. Murray and D. E. Burmaster, Residential air exchange rates in the united states: empirical and estimated parametric distributions by season and climatic region, *Risk Anal.*, 1995, **15**, 459–465.

6 S. K. Brown, M. R. Sim, M. J. Abramson and C. N. Gray, Concentrations of Volatile Organic Compounds in Indoor Air – A Review, *Indoor Air*, 1994, **4**, 123–134.

7 L. A. Wallace, E. D. Pellizzari, T. D. Hartwell, C. M. Sparacino, L. S. Sheldon and H. Zelon, Personal exposures, indoor-outdoor relationships, and breath levels of toxic air pollutants measured for 355 persons in New Jersey, *Atmos. Environ.*, 1985, **19**, 1651–1661.

8 L. A. Wallace, E. Pellizzari, B. Leaderer, H. Zelon and L. Sheldon, Emissions of volatile organic compounds from building materials and consumer products, *Atmos. Environ.*, 1987, **21**, 385–393.

9 C. J. Weschler, Roles of the human occupant in indoor chemistry, *Indoor Air*, 2016, **26**, 6–24.

10 S. Liu, R. Li, R. J. Wild, C. Warneke, J. A. de Gouw, S. S. Brown, S. L. Miller, J. C. Luongo, J. L. Jimenez and P. J. Ziemann, Contribution of human-related sources to indoor volatile organic compounds in a university classroom, *Indoor Air*, 2016, **26**, 925–938.

11 K. Kristensen, D. M. Lunderberg, Y. Liu, P. K. Misztal, Y. Tian, C. Arata, W. W. Nazaroff and A. H. Goldstein, Sources and dynamics of semivolatile organic compounds in a single-family residence in northern California, *Indoor Air*, 2019, **29**, 645–655.

12 A. L. Clobes, G. P. Ananth, A. L. Hood, J. A. Schroeder and K. A. Lee, Human activities as sources of volatile organic compounds in residential environments, *Ann. N. Y. Acad. Sci.*, 1992, **641**, 79–86.

13 A. Manuja, J. Ritchie, K. Buch, Y. Wu, C. M. A. Eichler, J. C. Little and L. C. Marr, Total surface area in indoor environments, *Environ. Sci.: Processes Impacts*, 2019, **21**, 1384–1392.

14 C. Wang, D. B. Collins, C. Arata, A. H. Goldstein, J. M. Mattila, D. K. Farmer, L. Ampollini, P. F. DeCarlo, A. Novoselac, M. E. Vance, W. W. Nazaroff and J. P. D. Abbatt, Surface reservoirs dominate dynamic gas-surface partitioning of many indoor air constituents, *Sci. Adv.*, 2020, **6**, eaay8973.

15 C. J. Weschler and W. W. Nazaroff, Semivolatile organic compounds in indoor environments, *Atmos. Environ.*, 2008, **42**, 9018–9040.

16 W. W. Nazaroff and C. J. Weschler, Indoor ozone: Concentrations and influencing factors, *Indoor Air*, 2022, **32**, e12942.

17 M. Sleiman, L. A. Gundel, J. F. Pankow, P. Jacob, B. C. Singer and H. Destaillats, Formation of carcinogens indoors by surface-mediated reactions of nicotine with nitrous acid, leading to potential thirdhand smoke hazards, *Proc. Natl. Acad. Sci. U. S. A.*, 2010, **107**, 6576–6581.

18 J. Liu, H. Deng, P. S. J. Lakey, H. Jiang, M. Mekic, X. Wang, M. Shiraiwa and S. Gligorovski, Unexpectedly High Indoor HONO Concentrations Associated with Photochemical NO2 Transformation on Glass Windows, *Environ. Sci. Technol.*, 2020, **54**, 15680–15688.

19 National Academies of Sciences, *Engineering, and Medicine; Division on Earth and Life Studies; Board on Chemical Sciences and Technology; Committee on Emerging Science on Indoor Chemistry, Why Indoor Chemistry Matters*, National Academies Press (US), Washington (DC), 2022.

20 C. J. Weschler and W. W. Nazaroff, Growth of organic films on indoor surfaces, *Indoor Air*, 2017, **27**, 1101–1112.

21 V. W. Or, M. R. Alves, M. Wade, S. Schwab, R. L. Corsi and V. H. Grassian, Crystal clear? microspectroscopic imaging and physicochemical characterization of indoor depositions on window glass, *Environ. Sci. Technol. Lett.*, 2018, **5**, 514–519.

22 H. Schwartz-Narbonne and D. J. Donaldson, Water uptake by indoor surface films, *Sci. Rep.*, 2019, **9**, 11089.

23 C. Y. Lim and J. P. Abbatt, Chemical composition, spatial homogeneity, and growth of indoor surface films, *Environ. Sci. Technol.*, 2020, **54**, 14372–14379.
24 Q.-T. Liu, R. Chen, B. E. McCarry, M. L. Diamond and B. Bahavar, Characterization of polar organic compounds in the organic film on indoor and outdoor glass windows, *Environ. Sci. Technol.*, 2003, **37**, 2340–2349.
25 M. Springs, J. R. Wells and G. C. Morrison, Reaction rates of ozone and terpenes adsorbed to model indoor surfaces, *Indoor Air*, 2011, **21**, 319–327.
26 L. Petrick and Y. Dubowski, Heterogeneous oxidation of squalene film by ozone under various indoor conditions, *Indoor Air*, 2009, **19**, 381–391.
27 G. Sarwar and R. Corsi, The effects of ozone/limonene reactions on indoor secondary organic aerosols, *Atmos. Environ.*, 2007, **41**, 959–973.
28 H. Destaillats, M. M. Lunden, B. C. Singer, B. K. Coleman, A. T. Hodgson, C. J. Weschler and W. W. Nazaroff, Indoor secondary pollutants from household product emissions in the presence of ozone: A bench-scale chamber study, *Environ. Sci. Technol.*, 2006, **40**, 4421–4428.
29 V. W. Or, M. R. Alves, M. Wade, S. Schwab, R. L. Corsi and V. H. Grassian, Nanoscopic Study of Water Uptake on Glass Surfaces with Organic Thin Films and Particles from Exposure to Indoor Cooking Activities: Comparison to Model Systems, *Environ. Sci. Technol.*, 2022, **56**, 1594–1604.
30 S. M. Duncan, K. Sexton, L. Collins and B. J. Turpin, Residential water-soluble organic gases: chemical characterization of a substantial contributor to indoor exposures, *Environ. Sci.: Processes Impacts*, 2019, **21**, 1364–1373.
31 S. M. Duncan, S. Tomaz, G. Morrison, M. Webb, J. Atkin, J. D. Surratt and B. J. Turpin, Dynamics of Residential Water-Soluble Organic Gases: Insights into Sources and Sinks, *Environ. Sci. Technol.*, 2019, **53**, 1812–1821.
32 R. Sander, Compilation of Henry's law constants (version 4.0) for water as solvent, *Atmos. Chem. Phys.*, 2015, **15**, 4399–4981.
33 D. Pagonis, D. J. Price, L. B. Algrim, D. A. Day, A. V. Handschy, H. Stark, S. L. Miller, J. de Gouw, J. L. Jimenez and P. J. Ziemann, Time-Resolved Measurements of Indoor Chemical Emissions, Deposition, and Reactions in a University Art Museum, *Environ. Sci. Technol.*, 2019, **53**, 4794–4802.
34 K. S. Docherty, W. Wu, Y. B. Lim and P. J. Ziemann, Contributions of Organic Peroxides to Secondary Aerosol Formed from Reactions of Monoterpenes with O3, *Environ. Sci. Technol.*, 2005, **39**, 4049–4059.
35 P. J. Ziemann, Evidence for Low-Volatility Diacyl Peroxides as a Nucleating Agent and Major Component of Aerosol Formed from Reactions of O3 with Cyclohexene and Homologous Compounds, *J. Phys. Chem. A*, 2002, **106**, 4390–4402.
36 S. Zhou, Z. Liu, Z. Wang, C. J. Young, T. C. VandenBoer, B. B. Guo, J. Zhang, N. Carslaw and T. F. Kahan, Hydrogen Peroxide Emission and Fate Indoors during Non-bleach Cleaning: A Chamber and Modeling Study, *Environ. Sci. Technol.*, 2020, **54**, 15643–15651.
37 E. Dovrou, J. C. Rivera-Rios, K. H. Bates and F. N. Keutsch, Sulfate Formation *via* Cloud Processing from Isoprene Hydroxyl Hydroperoxides (ISOPOOH), *Environ. Sci. Technol.*, 2019, **53**, 12476–12484.
38 D. W. O'Sullivan, M. Lee, B. C. Noone and B. G. Heikes, Henry's law constant determinations for hydrogen peroxide, methyl hydroperoxide, hydroxymethyl hydroperoxide, ethyl hydroperoxide, and peroxyacetic acid, *J. Phys. Chem.*, 1996, **100**, 3241–3247.
39 J. C. Rivera-Ríos, Atmospheric chemistry of isoprene hydroxyhydroperoxides, *Doctoral dissertation*, Harvard University, 2018.
40 Y. Zhang, L. Nichman, P. Spencer, J. I. Jung, A. Lee, B. K. Heffernan, A. Gold, Z. Zhang, Y. Chen, M. R. Canagaratna, J. T. Jayne, D. R. Worsnop, T. B. Onasch, J. D. Surratt, D. Chandler, P. Davidovits and C. E. Kolb, The Cooling Rate- and Volatility-Dependent Glass-Forming Properties of Organic Aerosols Measured by Broadband Dielectric Spectroscopy, *Environ. Sci. Technol.*, 2019, **53**, 12366–12378.
41 J. C. Rivera-Rios, T. B. Nguyen, J. D. Crounse, W. Jud, J. M. St. Clair, T. Mikoviny, J. B. Gilman, B. M. Lerner, J. B. Kaiser, J. de Gouw, A. Wisthaler, A. Hansel, P. O. Wennberg, J. H. Seinfeld and F. N. Keutsch, Conversion of hydroperoxides to carbonyls in field and laboratory instrumentation: Observational bias in diagnosing pristine *versus* anthropogenically controlled atmospheric chemistry, *Geophys. Res. Lett.*, 2014, **41**, 8645–8651.
42 S. Inomata, K. Sato, J. Hirokawa, Y. Sakamoto, H. Tanimoto, M. Okumura, S. Tohno and T. Imamura, Analysis of secondary organic aerosols from ozonolysis of isoprene by proton transfer reaction mass spectrometry, *Atmos. Environ.*, 2014, **97**, 397–405.
43 D. H. Bennett and E. J. Furtaw, Fugacity-based indoor residential pesticide fate model, *Environ. Sci. Technol.*, 2004, **38**, 2142–2152.
44 D. Huang, Z. M. Chen, Y. Zhao and H. Liang, Newly observed peroxides and the water effect on the formation and removal of hydroxyalkyl hydroperoxides in the ozonolysis of isoprene, *Atmos. Chem. Phys.*, 2013, **13**, 5671–5683.
45 Z. Fan, C. J. Weschler, I.-K. Han and J. J. Zhang, Co-formation of hydroperoxides and ultra-fine particles during the reactions of ozone with a complex VOC mixture under simulated indoor conditions, *Atmos. Environ.*, 2005, **39**, 5171–5182.
46 T.-H. Li, B. J. Turpin, H. C. Shields and C. J. Weschler, Indoor hydrogen peroxide derived from ozone/d-limonene reactions, *Environ. Sci. Technol.*, 2002, **36**, 3295–3302.
47 M. Riva, S. H. Budisulistiorini, Z. Zhang, A. Gold and J. D. Surratt, Chemical characterization of secondary organic aerosol constituents from isoprene ozonolysis in the presence of acidic aerosol, *Atmos. Environ.*, 2016, **130**, 5–13.

 

48 N. Carslaw, A mechanistic study of limonene oxidation products and pathways following cleaning activities, *Atmos. Environ.*, 2013, **80**, 507–513.
49 P. Venkatachari and P. K. Hopke, Development and Laboratory Testing of an Automated Monitor for the Measurement of Atmospheric Particle-Bound Reactive Oxygen Species (ROS), *Aerosol Sci. Technol.*, 2008, **42**, 629–635.
50 G. C. Morrison, A. Eftekhari, P. S. J. Lakey, M. Shiraiwa, B. E. Cummings, M. S. Waring and B. Williams, Partitioning of reactive oxygen species from indoor surfaces to indoor aerosols, *Environ. Sci.: Processes Impacts*, 2022, **24**, 2310–2323.
51 N. Carslaw, T. Mota, M. E. Jenkin, M. H. Barley and G. McFiggans, A significant role for nitrate and peroxide groups on indoor secondary organic aerosol, *Environ. Sci. Technol.*, 2012, **46**, 9290–9298.
52 S. Enami, Fates of organic hydroperoxides in atmospheric condensed phases, *J. Phys. Chem. A*, 2021, **125**, 4513–4523.
53 H. Li, Z. Chen, L. Huang and D. Huang, Organic peroxides' gas-particle partitioning and rapid heterogeneous decomposition on secondary organic aerosol, *Atmos. Chem. Phys.*, 2016, **16**, 1837–1848.
54 Y. B. Lim and B. J. Turpin, Laboratory evidence of organic peroxide and peroxyhemiacetal formation in the aqueous phase and implications for aqueous OH, *Atmos. Chem. Phys.*, 2015, **15**, 12867–12877.
55 M. Riva, S. H. Budisulistiorini, Z. Zhang, A. Gold, J. A. Thornton, B. J. Turpin and J. D. Surratt, Multiphase reactivity of gaseous hydroperoxide oligomers produced from isoprene ozonolysis in the presence of acidified aerosols, *Atmos. Environ.*, 2017, **152**, 314–322.
56 L. Poulain, A. Tilgner, M. Brüggemann, P. Mettke, L. He, J. Anders, O. Böge, A. Mutzel and H. Herrmann, Particle-phase uptake and chemistry of highly oxygenated organic molecules (homs) from α-pinene OH oxidation, *J. Geophys. Res.*, 2022, **127**(1627), e2021JD036414.
57 H. O. T. Pye, A. Nenes, B. Alexander, A. P. Ault, M. C. Barth, S. L. Clegg, J. L. Collett Jr, K. M. Fahey, C. J. Hennigan, H. Herrmann, M. Kanakidou, J. T. Kelly, I.-T. Ku, V. F. McNeill, N. Riemer, T. Schaefer, G. Shi, A. Tilgner, J. T. Walker, T. Wang, R. Weber, J. Xing, R. A. Zaveri and A. Zuend, The acidity of atmospheric particles and clouds, *Atmos. Chem. Phys.*, 2020, **20**, 4809–4888.
58 W. W. Nazaroff and C. J. Weschler, Indoor acids and bases, *Indoor Air*, 2020, **30**, 559–644.
59 J. L. Nguyen, J. Schwartz and D. W. Dockery, The relationship between indoor and outdoor temperature, apparent temperature, relative humidity, and absolute humidity, *Indoor Air*, 2014, **24**, 103–112.
60 J. A. Cano-Ruiz, D. Kong, R. B. Balas and W. W. Nazaroff, Removal of reactive gases at indoor surfaces: Combining mass transport and surface kinetics, *Atmos. Environ., Part A*, 1993, **27**, 2039–2050.
61 W. W. Nazaroff, A. J. Gadgil and C. J. Weschler, Critique of the use of deposition velocity in modeling indoor air quality, *Modeling of indoor Air Quality and Exposure, ASTM STP 1205*, ed. N. L. Nagda, American Society for Testing and Materials, Philadelphia, 1993, pp. 81–104.
62 G. Bekö, N. Carslaw, P. Fauser, V. Kauneliene, S. Nehr, G. Phillips, D. Saraga, C. Schoemaecker, A. Wierzbicka and X. Querol, The past, present, and future of indoor air chemistry, *Indoor Air*, 2020, **30**, 373–376.
63 N. Carslaw, A new detailed chemical model for indoor air pollution, *Atmos. Environ.*, 2007, **41**, 1164–1179.
64 T. P. Riedel, Y.-H. Lin, S. H. Budisulistiorini, C. J. Gaston, J. A. Thornton, Z. Zhang, W. Vizuete, A. Gold and J. D. Surratt, Heterogeneous Reactions of Isoprene-Derived Epoxides: Reaction Probabilities and Molar Secondary Organic Aerosol Yield Estimates, *Environ. Sci. Technol. Lett.*, 2015, **2**, 38–42.
65 C. J. Gaston, T. P. Riedel, Z. Zhang, A. Gold, J. D. Surratt and J. A. Thornton, Reactive uptake of an isoprene-derived epoxydiol to submicron aerosol particles, *Environ. Sci. Technol.*, 2014, **48**, 11178–11186.
66 J. A. Thornton, C. F. Braban and J. P. D. Abbatt, N2O5 hydrolysis on sub-micron organic aerosols: the effect of relative humidity, particle phase, and particle size, *Phys. Chem. Chem. Phys.*, 2003, **5**, 4593.
67 T. H. Bertram, J. A. Thornton and T. P. Riedel, An experimental technique for the direct measurement of N2O5 reactivity on ambient particles, *Atmos. Meas. Tech.*, 2009, **2**, 231–242.
68 J. Shang, M. Passananti, Y. Dupart, R. Ciuraru, L. Tinel, S. Rossignol, S. Perrier, T. Zhu and C. George, SO2 uptake on oleic acid: A new formation pathway of organosulfur compounds in the atmosphere, *Environ. Sci. Technol. Lett.*, 2016, **3**, 67–72.
69 D. Zhang and R. Zhang, Laboratory Investigation of Heterogeneous Interaction of Sulfuric Acid with Soot, *Environ. Sci. Technol.*, 2005, **39**, 5722–5728.
70 M. Riva, S. H. Budisulistiorini, Y. Chen, Z. Zhang, E. L. D'Ambro, X. Zhang, A. Gold, B. J. Turpin, J. A. Thornton, M. R. Canagaratna and J. D. Surratt, Chemical Characterization of Secondary Organic Aerosol from Oxidation of Isoprene Hydroxyhydroperoxides, *Environ. Sci. Technol.*, 2016, **50**, 9889–9899.
71 Y. Zhang, Y. Chen, A. T. Lambe, N. E. Olson, Z. Lei, R. L. Craig, Z. Zhang, A. Gold, T. B. Onasch, J. T. Jayne, D. R. Worsnop, C. J. Gaston, J. A. Thornton, W. Vizuete, A. P. Ault and J. D. Surratt, Effect of the Aerosol-Phase State on Secondary Organic Aerosol Formation from the Reactive Uptake of Isoprene-Derived Epoxydiols (IEPOX), *Environ. Sci. Technol. Lett.*, 2018, **5**, 167–174.
72 W. C. Hinds and Y. Zhu, *Aerosol Technology: Properties, Behavior, and Measurement of Airborne Particles*, John Wiley & Sons, 2022.
73 L. Cui, A parallel plate reactor built with wall materials for indoor surface chemistry study, *Master thesis*, University of North Carolina at Chapel Hill, 2019.
74 P. G. Gormley, Diffusion from a stream flowing through a thin rectangular tube, *Proc. R. Ir. Acad.*, 1938, **45**, 59.

75 S. S. Parmar and D. Grosjean, Laboratory tests of KI and alkaline annular denuders, *Atmos. Environ., Part A*, 1990, **24**, 2695–2698.
76 S. P. Lamble, R. L. Corsi and G. C. Morrison, Ozone deposition velocities, reaction probabilities and product yields for green building materials, *Atmos. Environ.*, 2011, **45**, 6965–6972.
77 G. C. Morrison and W. W. Nazaroff, The rate of ozone uptake on carpets: experimental studies, *Environ. Sci. Technol.*, 2000, **34**, 4963–4968.
78 H. Wang and G. Morrison, Ozone-surface reactions in five homes: surface reaction probabilities, aldehyde yields, and trends, *Indoor Air*, 2010, **20**, 224–234.
79 P. O. Wennberg, K. H. Bates, J. D. Crounse, L. G. Dodson, R. C. McVay, L. A. Mertens, T. B. Nguyen, E. Praske, R. H. Schwantes, M. D. Smarte, J. M. St Clair, A. P. Teng, X. Zhang and J. H. Seinfeld, Gas-Phase Reactions of Isoprene and Its Major Oxidation Products, *Chem. Rev.*, 2018, **118**, 3337–3390.
80 J. M. St Clair, J. C. Rivera-Rios, J. D. Crounse, H. C. Knap, K. H. Bates, A. P. Teng, S. Jørgensen, H. G. Kjaergaard, F. N. Keutsch and P. O. Wennberg, Kinetics and Products of the Reaction of the First-Generation Isoprene Hydroxy Hydroperoxide (ISOPOOH) with OH, *J. Phys. Chem. A*, 2016, **120**, 1441–1451.
81 F. Paulot, J. D. Crounse, H. G. Kjaergaard, A. Kürten, J. M. St Clair, J. H. Seinfeld and P. O. Wennberg, Unexpected epoxide formation in the gas-phase photooxidation of isoprene, *Science*, 2009, **325**, 730–733.
82 A. Guenther, T. Karl, P. Harley, C. Wiedinmyer, P. I. Palmer and C. Geron, Estimates of global terrestrial isoprene emissions using MEGAN (Model of Emissions of Gases and Aerosols from Nature), *Atmos. Chem. Phys.*, 2006, **6**, 3181–3210.
83 E. T. Gall and D. Rim, Mass accretion and ozone reactivity of idealized indoor surfaces in mechanically or naturally ventilated indoor environments, *Build. Environ.*, 2018, **138**, 89–97.
84 T. Grøntoft and M. R. Raychaudhuri, Compilation of tables of surface deposition velocities for $O_3$, $NO_2$ and $SO_2$ to a range of indoor surfaces, *Atmos. Environ.*, 2004, **38**, 533–544.
85 J. Shen and Z. Gao, Ozone removal on building material surface: A literature review, *Build. Environ.*, 2018, **134**, 205–217.
86 E. Dovrou, K. H. Bates, J. C. Rivera-Rios, J. L. Cox, J. D. Shutter and F. N. Keutsch, Towards a chemical mechanism of the oxidation of aqueous sulfur dioxide *via* isoprene hydroxyl hydroperoxides (ISOPOOH), *Atmos. Chem. Phys.*, 2021, **21**, 8999–9008.
87 W. W. Nazaroff and G. R. Cass, Mathematical modeling of chemically reactive pollutants in indoor air, *Environ. Sci. Technol.*, 1986, **20**, 924–934.
88 G. Sarwar, R. Corsi, Y. Kimura, D. Allen and C. J. Weschler, Hydroxyl radicals in indoor environments, *Atmos. Environ.*, 2002, **36**, 3973–3988.
89 B. L. Deming and P. J. Ziemann, Quantification of alkenes on indoor surfaces and implications for chemical sources and sinks, *Indoor Air*, 2020, **30**, 914–924.
90 Y. Wu, C. M. A. Eichler, W. Leng, S. S. Cox, L. C. Marr and J. C. Little, Adsorption of phthalates on impervious indoor surfaces, *Environ. Sci. Technol.*, 2017, **51**, 2907–2913.
91 W. Gao, J. Wu, Y. Wang and G. Jiang, Distribution and congener profiles of short-chain chlorinated paraffins in indoor/outdoor glass window surface films and their film-air partitioning in Beijing, China, *Chemosphere*, 2016, **144**, 1327–1333.
92 J. Li, T. Lin, S.-H. Pan, Y. Xu, X. Liu, G. Zhang and X.-D. Li, Carbonaceous matter and PBDEs on indoor/outdoor glass window surfaces in Guangzhou and Hong Kong, South China, *Atmos. Environ.*, 2010, **44**, 3254–3260.
93 S. Wang, Y. Zhao, A. W. H. Chan, M. Yao, Z. Chen and J. P. D. Abbatt, Organic peroxides in aerosol: key reactive intermediates for multiphase processes in the atmosphere, *Chem. Rev.*, 2023, **123**, 1635–1679.
94 S. Wang, S. Zhou, Y. Tao, W. G. Tsui, J. Ye, J. Z. Yu, J. G. Murphy, V. F. McNeill, J. P. D. Abbatt and A. W. H. Chan, Organic peroxides and sulfur dioxide in aerosol: source of particulate sulfate, *Environ. Sci. Technol.*, 2019, **53**, 10695–10704.
95 Y. Liu, M. Kuwata, K. A. McKinney and S. T. Martin, Uptake and release of gaseous species accompanying the reactions of isoprene photo-oxidation products with sulfate particles, *Phys. Chem. Chem. Phys.*, 2016, **18**, 1595–1600.
96 J. Qiu, K. Tonokura and S. Enami, Proton-Catalyzed Decomposition of α-Hydroxyalkyl-Hydroperoxides in Water, *Environ. Sci. Technol.*, 2020, **54**, 10561–10569.
97 H. Tong, A. M. Arangio, P. S. J. Lakey, T. Berkemeier, F. Liu, C. J. Kampf, W. H. Brune, U. Pöschl and M. Shiraiwa, Hydroxyl radicals from secondary organic aerosol decomposition in water, *Atmos. Chem. Phys.*, 2016, **16**, 1761–1771.
98 K. M. Badali, S. Zhou, D. Aljawhary, M. Antiñolo, W. J. Chen, A. Lok, E. Mungall, J. P. S. Wong, R. Zhao and J. P. D. Abbatt, Formation of hydroxyl radicals from photolysis of secondary organic aerosol material, *Atmos. Chem. Phys.*, 2015, **15**, 7831–7840.
99 T. Fang, P. S. J. Lakey, J. C. Rivera-Rios, F. N. Keutsch and M. Shiraiwa, Aqueous-Phase Decomposition of Isoprene Hydroxy Hydroperoxide and Hydroxyl Radical Formation by Fenton-like Reactions with Iron Ions, *J. Phys. Chem. A*, 2020, **124**, 5230–5236.
100 Y. B. Lim, Y. Tan, M. J. Perri, S. P. Seitzinger and B. J. Turpin, Aqueous chemistry and its role in secondary organic aerosol (SOA) formation, *Atmos. Chem. Phys.*, 2010, **10**, 10521–10539.
101 M. Lee, B. G. Heikes and D. W. O'Sullivan, Hydrogen peroxide and organic hydroperoxide in the troposphere: a review, *Atmos. Environ.*, 2000, **34**, 3475–3494.
102 Y. Sakamoto, S. Inomata and J. Hirokawa, Oligomerization reaction of the Criegee intermediate leads to secondary organic aerosol formation in ethylene ozonolysis, *J. Phys. Chem. A*, 2013, **117**, 12912–12921.

 

103 B. Chu, Y. Liu, J. Li, H. Takekawa, J. Liggio, S.-M. Li, J. Jiang, J. Hao and H. He, Decreasing effect and mechanism of FeSO4 seed particles on secondary organic aerosol in α-pinene photooxidation, *Environ. Pollut.*, 2014, **193**, 88–93.
104 S. F. Kowal, S. R. Allen and T. F. Kahan, Wavelength-Resolved Photon Fluxes of Indoor Light Sources: Implications for HOx Production, *Environ. Sci. Technol.*, 2017, **51**, 10423–10430.
105 M. N. Rashed, Total and Extractable Heavy Metals in Indoor, Outdoor and Street Dust from Aswan City, Egypt, *Clean: Soil, Air, Water*, 2008, **36**, 850–857.
106 L. Zhou, G. Liu, M. Shen and Y. Liu, Potential ecological and health risks of heavy metals for indoor and corresponding outdoor dust in Hefei, Central China, *Chemosphere*, 2022, **302**, 134864.
107 D. Pagonis and P. J. Ziemann, Chemistry of hydroperoxycarbonyls in secondary organic aerosol, *Aerosol Sci. Technol.*, 2018, **52**, 1178–1193.
108 M. Krapf, I. El Haddad, E. A. Bruns, U. Molteni, K. R. Daellenbach, A. S. H. Prévôt, U. Baltensperger and J. Dommen, Labile peroxides in secondary organic aerosol, *Chem*, 2016, **1**, 603–616.
109 H. Herrmann, A. Tilgner, P. Barzaghi, Z. Majdik, S. Gligorovski, L. Poulain and A. Monod, Towards a more detailed description of tropospheric aqueous phase organic chemistry: CAPRAM 3.0, *Atmos. Environ.*, 2005, **39**, 4351–4363.
110 L. Deguillaume, M. Leriche, K. Desboeufs, G. Mailhot, C. George and N. Chaumerliac, Transition metals in atmospheric liquid phases: sources, reactivity, and sensitive parameters, *Chem. Rev.*, 2005, **105**, 3388–3431.
111 J. De Laat and T. G. Le, Effects of chloride ions on the iron(III)-catalyzed decomposition of hydrogen peroxide and on the efficiency of the Fenton-like oxidation process, *Appl. Catal., B*, 2006, **66**, 137–146.
112 J. Honzíček, Curing of Air-Drying Paints: A Critical Review, *Ind. Eng. Chem. Res.*, 2019, **58**, 12485–12505.
113 L. Morawska, A. Afshari, G. N. Bae, G. Buonanno, C. Y. H. Chao, O. Hänninen, W. Hofmann, C. Isaxon, E. R. Jayaratne, P. Pasanen, T. Salthammer, M. Waring and A. Wierzbicka, Indoor aerosols: from personal exposure to risk assessment, *Indoor Air*, 2013, **23**, 462–487.
114 Y. B. Lim, Y. Tan and B. J. Turpin, Chemical insights, explicit chemistry, and yields of secondary organic aerosol from OH radical oxidation of methylglyoxal and glyoxal in the aqueous phase, *Atmos. Chem. Phys.*, 2013, **13**, 8651–8667.
115 V. F. McNeill, Aqueous organic chemistry in the atmosphere: sources and chemical processing of organic aerosols, *Environ. Sci. Technol.*, 2015, **49**, 1237–1244.
116 J. Qiu, S. Ishizuka, K. Tonokura, A. J. Colussi and S. Enami, Water Dramatically Accelerates the Decomposition of α-Hydroxyalkyl-Hydroperoxides in Aerosol Particles, *J. Phys. Chem. Lett.*, 2019, **10**, 5748–5755.
117 B. H. Lee, F. D. Lopez-Hilfiker, C. Mohr, T. Kurtén, D. R. Worsnop and J. A. Thornton, An iodide-adduct high-resolution time-of-flight chemical-ionization mass spectrometer: application to atmospheric inorganic and organic compounds, *Environ. Sci. Technol.*, 2014, **48**, 6309–6317.
118 M. Ongwandee and P. Sawanyapanich, Influence of relative humidity and gaseous ammonia on the nicotine sorption to indoor materials, *Indoor Air*, 2012, **22**, 54–63.
119 W. C. Keene, A. A. P. Pszenny, J. R. Maben, E. Stevenson and A. Wall, Closure evaluation of size-resolved aerosol pH in the New England coastal atmosphere during summer, *J. Geophys. Res. Atmos.*, 2004, **109**(D23), D2316.
120 M. Brauer, P. Koutrakis, G. J. Keeler and J. D. Spengler, Indoor and outdoor concentrations of inorganic acidic aerosols and gases, *J. Air Waste Manage. Assoc.*, 1991, **41**, 171–181.
121 C. S. K. Liang and J. M. Waldman, Indoor exposures to acidic aerosols at child and elderly care facilities, *Indoor Air*, 1992, **2**, 196–207.
122 H. Guo, L. Xu, A. Bougiatioti, K. M. Cerully, S. L. Capps, J. R. Hite, A. G. Carlton, S. H. Lee, M. H. Bergin, N. L. Ng, A. Nenes and R. J. Weber, Fine-particle water and pH in the southeastern United States, *Atmos. Chem. Phys.*, 2015, **15**, 5211–5228.
123 V. W. Or, M. Wade, S. Patel, M. R. Alves, D. Kim, S. Schwab, H. Przelomski, R. O'Brien, D. Rim, R. L. Corsi, M. E. Vance, D. K. Farmer and V. H. Grassian, Glass surface evolution following gas adsorption and particle deposition from indoor cooking events as probed by microspectroscopic analysis, *Environ. Sci.: Processes Impacts*, 2020, **22**, 1698–1709.
124 T. Liu, A. W. H. Chan and J. P. D. Abbatt, Multiphase oxidation of sulfur dioxide in aerosol particles: implications for sulfate formation in polluted environments, *Environ. Sci. Technol.*, 2021, **55**, 4227–4242.
125 D. Vione, V. Maurino, C. Minero and E. Pelizzetti, The atmospheric chemistry of hydrogen peroxide: a review, *Ann. Chim.*, 2003, **93**, 477–488.
126 J. A. Lind, A. L. Lazrus and G. L. Kok, Aqueous phase oxidation of sulfur(IV) by hydrogen peroxide, methylhydroperoxide, and peroxyacetic acid, *J. Geophys. Res.*, 1987, **92**, 4171.
127 J. Ye, J. P. D. Abbatt and A. W. H. Chan, Novel pathway of SO2 oxidation in the atmosphere: reactions with monoterpene ozonolysis intermediates and secondary organic aerosol, *Atmos. Chem. Phys.*, 2018, **18**, 5549–5565.
128 H. J. Tobias and P. J. Ziemann, Thermal Desorption Mass Spectrometric Analysis of Organic Aerosol Formed from Reactions of 1-Tetradecene and O3 in the Presence of Alcohols and Carboxylic Acids, *Environ. Sci. Technol.*, 2000, **34**, 2105–2115.
129 M. Kruza, A. C. Lewis, G. C. Morrison and N. Carslaw, Impact of surface ozone interactions on indoor air chemistry: A modeling study, *Indoor Air*, 2017, **27**, 1001–1011.
130 A. T. Hodgson, D. Beal and J. E. R. McIlvaine, Sources of formaldehyde, other aldehydes and terpenes in a new manufactured house, *Indoor Air*, 2002, **12**, 235–242.

131 F. Klein, U. Baltensperger, A. S. H. Prévôt and I. El Haddad, Quantification of the impact of cooking processes on indoor concentrations of volatile organic species and primary and secondary organic aerosols, *Indoor Air*, 2019, **29**, 926–942.

132 J. Zhang, P. J. Lioy and Q. He, Characteristics of aldehydes: concentrations, sources, and exposures for indoor and outdoor residential microenvironments, *Environ. Sci. Technol.*, 1994, **28**, 146–152.

133 A. T. Hodgson, K. Y. Ming and B. C. Singer, *Quantifying Object and Material Surface Areas in Residences*, Lawrence Berkeley National Laboratory (LBNL), Berkeley, CA, 2005.

134 C. J. Weschler, Ozone in indoor environments: concentration and chemistry, *Indoor Air*, 2000, **10**, 269–288.

135 W. W. Nazaroff, Residential air-change rates: A critical review, *Indoor Air*, 2021, **31**, 282–313.

136 R. H. Sabersky, D. A. Sinema and F. H. Shair, Concentrations, decay rates, and removal of ozone and their relation to establishing clean indoor air, *Environ. Sci. Technol.*, 1973, **7**, 347–353.

137 F. X. Mueller, L. Loeb and W. H. Mapes, Decomposition rates of ozone in living areas, *Environ. Sci. Technol.*, 1973, **7**, 342–346.

138 Y. Liu, P. K. Misztal, C. Arata, C. J. Weschler, W. W. Nazaroff and A. H. Goldstein, Observing ozone chemistry in an occupied residence, *Proc. Natl. Acad. Sci. U. S. A.*, 2021, **118**, e2018140118.

139 K. Lee, J. Vallarino, T. Dumyahn, H. Ozkaynak and J. D. Spengler, Ozone decay rates in residences, *J. Air Waste Manage. Assoc.*, 1999, **49**, 1238–1244.

140 M. N. Romanias, A. El Zein and Y. Bedjanian, Heterogeneous interaction of H2O2 with TiO2 surface under dark and UV light irradiation conditions, *J. Phys. Chem. A*, 2012, **116**, 8191–8200.

141 J. A. Snow, Winter-spring evolution and variability of HOx reservoir species, hydrogen peroxide, and methyl hydroperoxide, in the northern middle to high latitudes, *J. Geophys. Res.*, 2003, **108**, 8362.

142 J. D. Crounse, K. A. McKinney, A. J. Kwan and P. O. Wennberg, Measurement of gas-phase hydroperoxides by chemical ionization mass spectrometry, *Anal. Chem.*, 2006, **78**, 6726–6732.

143 J. E. Krechmer, M. M. Coggon, P. Massoli, T. B. Nguyen, J. D. Crounse, W. Hu, D. A. Day, G. S. Tyndall, D. K. Henze, J. C. Rivera-Rios, J. B. Nowak, J. R. Kimmel, R. L. Mauldin, H. Stark, J. T. Jayne, M. Sipilä, H. Junninen, J. M. S. Clair, X. Zhang, P. A. Feiner, L. Zhang, D. O. Miller, W. H. Brune, F. N. Keutsch, P. O. Wennberg, J. H. Seinfeld, D. R. Worsnop, J. L. Jimenez and M. R. Canagaratna, Formation of Low Volatility Organic Compounds and Secondary Organic Aerosol from Isoprene Hydroxyhydroperoxide Low-NO Oxidation, *Environ. Sci. Technol.*, 2015, **49**, 10330–10339.

144 H. Tong, Y. Zhang, A. Filippi, T. Wang, C. Li, F. Liu, D. Leppla, I. Kourtchev, K. Wang, H.-M. Keskinen, J. T. Levula, A. M. Arangio, F. Shen, F. Ditas, S. T. Martin, P. Artaxo, R. H. M. Godoi, C. I. Yamamoto, R. A. F. de Souza, R.-J. Huang, T. Berkemeier, Y. Wang, H. Su, Y. Cheng, F. D. Pope, P. Fu, M. Yao, C. Pöhlker, T. Petäjä, M. Kulmala, M. O. Andreae, M. Shiraiwa, U. Pöschl, T. Hoffmann and M. Kalberer, Radical Formation by Fine Particulate Matter Associated with Highly Oxygenated Molecules, *Environ. Sci. Technol.*, 2019, **53**, 12506–12518.

145 W. W. Nazaroff and C. J. Weschler, Cleaning products and air fresheners: exposure to primary and secondary air pollutants, *Atmos. Environ.*, 2004, **38**, 2841–2865.

146 C. J. Weschler and N. Carslaw, Indoor Chemistry, *Environ. Sci. Technol.*, 2018, **52**, 2419–2428.

147 S. Batterman, J. Y. Chin, C. Jia, C. Godwin, E. Parker, T. Robins, P. Max and T. Lewis, Sources, concentrations, and risks of naphthalene in indoor and outdoor air, *Indoor Air*, 2012, **22**, 266–278.

148 M. Wang, S. Jia, S. H. Lee, A. Chow and M. Fang, Polycyclic aromatic hydrocarbons (PAHs) in indoor environments are still imposing carcinogenic risk, *J. Hazard. Mater.*, 2021, **409**, 124531.

149 R. Alwarda, S. Zhou and J. P. D. Abbatt, Heterogeneous oxidation of indoor surfaces by gas-phase hydroxyl radicals, *Indoor Air*, 2018, **28**, 655–664.

 